Current Research (2019) Newfoundland and Labrador Department of Natural Resources Geological Survey, Report 19-1, pages 59-83

THE AGS FLUORITE DEPOSIT, ST. LAWRENCE: PARAGENETIC SEQUENCE, FLUID-INCLUSION ANALYSIS, STRUCTURAL CONTROL, HOST ROCK GEOCHRONOLOGY AND IMPLICATIONS FOR ORE GENESIS

Z. Magyarosi, B.A. Sparkes[1], J. Conliffe and G.R. Dunning[2]
Mineral Deposits Section
[1]Canada Fluorspar (NL) Inc.
[2]Department of Earth Sciences, Memorial University of Newfoundland, St. John's, Newfoundland, A1B 3X5

ABSTRACT

The AGS deposit is the only known economically significant fluorite deposit in the St. Lawrence area not hosted entirely within the St. Lawrence Granite (SLG). The lack of economic fluorite deposits in the country rocks was historically explained by the notion that the sedimentary rocks were hornfelsed by the intrusion of the granite, thereby becoming impermeable to the mineralizing fluids, and/or that the fluorite being deposited in fissures formed as a result of cooling and contraction in the granite and that these fissures narrowed and closed as they entered the country rocks. The fluorite veins in the AGS area occur in sedimentary rocks and rhyolite sills that intrude them.

A sample of a rhyolite yielded a U–Pb zircon age slightly older than the main SLG (377.2 ± 1.3 Ma vs. the earlier published age of 374 ± 2 Ma for the main SLG), however, similarities in mineralogy and geochemistry of the sills and the SLG suggest that the former is a slightly earlier phase of the latter. Quartz, potassic feldspar and minor plagioclase form the phenocrysts and the groundmass in the rhyolite indicating two-stage cooling, with undercooling in the second stage. The rhyolite magma was likely separated from the granite because of a sudden pressure drop, and it intruded along fractures and faults to shallower levels, where it was rapidly quenched.

The fluorite veins are hosted in a well-developed, sinistral strike-slip fault. The process of fluorite crystallization is similar to the granite-hosted veins with repeated movement along the fault resulting in the brecciation of host rocks and pre-existing vein material, thus creating space for several successive phases of fluorite mineralization.

Fluorite mineralization is divided into three stages, which are further subdivided into ten phases. The early stage is represented by barren breccia, purple and yellow fluorite; the main stage by massive reddish grey and elongated grey fluorite separated by narrow bands of fine-grained sphalerite and minor galena; and the late stage by green, white and blue fluorite, followed by cubic blue or clear fluorite, late quartz or blastonite and minor pyrite and chalcopyrite. Calcite occurs in varying amounts in multiple phases of the deposit paragenetic sequence.

Fluid inclusion analysis indicate a trend from high salinity, lower temperature fluids to low salinity, slightly higher temperature fluids suggesting mixing of high-salinity magmatic fluid with low-salinity meteoric fluid.

The sequence of events that led to the formation of the AGS deposit is inferred as follows: 1) deposition of the Inlet Group sedimentary rocks; 2) faulting in the sediments; 3) emplacement of the rhyolite sills; and 4) emplacement of the underlying granite. The fault reactivated around the time of the intrusion of the SLG, which prevented ponding of the mineralizing fluids in the granite and provided channels for the fluids to migrate upward. The intrusion of the rhyolite further weakened the existing fault zone by volatiles escaping along the fault due to release in pressure.

INTRODUCTION

The AGS deposit is the most recent, and currently the only producing, fluorite mine in the St. Lawrence area. Fluorite occurs in veins hosted in sedimentary rocks and in rhyolite sills that intrude them, which is atypical in this area. Until recently, all veins associated with significant fluorite mineralization were thought to be typically hosted in the St. Lawrence Granite (SLG). A few peripheral veins have been identified, but no economic quantities of fluorite was associated with them.

Fluorite in the AGS area was first discovered by Newfoundland Fluorspar Ltd. (Newfluor) at the Open Cut Pit (west end of AGS vein system) in the late 1940s, and the occurrence was called the Grebes Nest (Smith, 1957; Sparkes and Reeves, 2015). This was followed by limited exploration producing mixed results. Since 2012, Canada Fluorspar (NL) Inc. (CFI) has carried out extensive exploration in the St. Lawrence area, including the AGS area (Sparkes and Reeves, 2015). In 2013, based on the results of geophysical surveys, drilling and trenching were undertaken, which resulted in the discovery of the AGS deposit.

This study is a multiyear project with the purpose of understanding the geological controls on the AGS deposit, which will help in more efficient mining, and further exploration for similar deposits in the area and elsewhere in the Province. In the first year, the project focused on the mineralogy, a preliminary paragenetic sequence and a comparison of the AGS veins with several granite-hosted veins (Magyarosi, 2018). In the second year, the project focused on the geochemistry and geochronology of the rhyolite sills, structural geology of the AGS veins, an updated paragenetic sequence and fluid inclusion analysis. This paper summarizes the results of the second year of the project.

GEOLOGICAL SETTING

REGIONAL GEOLOGY

Rocks in the St. Lawrence area are part of the Avalon Zone, which is the most easterly tectonostratigraphic component of the Appalachian orogeny in Newfoundland (Williams *et al.*, 1974; Williams, 1995; van Staal and Zagorevski, 2017; Figure 1). The Avalon Zone, as defined in North America, extends from eastern Newfoundland to North Georgia for approximately 3000 km (O'Brien *et al.*, 1998). Avalonian rocks correlate with the Caledonides in the United Kingdom, as well as with the rocks of the Pan African orogenic system. In Newfoundland, the Avalon Zone is approximately 600 km wide, extending from the Dover Fault in the west to the eastern boundary of the Grand Banks in the east.

The Avalon Zone consists of Neoproterozoic arc-related volcanic and sedimentary rocks that are fault-bounded and subjected to the Neoproterozoic Avalonian orogeny, resulting in folding, faulting, uplift and erosion (Williams *et al.*, 1974; Williams, 1995; Taylor, 1976; King, 1988; O'Brien *et al.*, 1996; van Staal and Zagorevski, 2017). The metamorphic grade is generally low, ranging up to lower-greenschist facies (Papezik, 1974). The Avalonian orogeny follows the deposition of the Cambrian–Early Ordovician platformal shales. The Avalon Zone is intruded by Late Precambrian and Late Devonian granites (Van Alstine, 1948; King, 1988; Krogh *et al.*, 1988). The Late Precambrian granites are calc-alkaline and intruded in arc and back-arc settings, followed by folding and thrust faulting and the intrusion of Late Devonian granites, including the SLG (O'Brien *et al.*, 1996).

LOCAL GEOLOGY

The first detailed mapping in the St. Lawrence area was completed by Strong *et al.* (1976, 1978) to the north, and O'Brien *et al.* (1977) to the south (Figure 2). Additional work by Hiscott (1981), Strong and Dostal (1980), O'Brien and Taylor (1983), Krogh *et al.* (1988), O'Brien *et al.* (1996, 1998) and O'Driscoll *et al.* (2001) helped in further understanding the geology of the area. The following provides an overview of the geology proceeding from the oldest rocks in the area to the youngest.

The Burin Group represents the oldest rocks in the area, dated using U–Pb isotopes in zircon, yielding an age of 765 +2.2/-1.8 Ma (Krogh *et al.*, 1988; Figure 2). It is composed of mafic volcanic rocks, minor clastic sedimentary rocks, limestone, gabbro sills and ultramafic rocks (Strong *et al.*, 1976, 1978; O'Driscoll *et al.*, 2001).

The Marystown Group is composed of felsic and mafic, dominantly pyroclastic rocks, volcaniclastic sedimentary and minor clastic sedimentary rocks (Figure 2). Dating by Sparkes and Dunning (2014) yielded ages between 576.8 ± 2.8 Ma and 574.4 ± 2.5 Ma.

The Musgravetown Group consists of a sequence of fining-upward clastic sedimentary rocks ranging from conglomerate to siltstone, and minor dolomitized limestone beds and clasts in conglomerate (Strong *et al.*, 1978; Hiscott, 1981; Figure 2). Age dating of a rhyolite from the upper portion of the Musgravetown Group yielded an age of 570 +5/-3 Ma (O'Brien *et al.*, 1989).

The Inlet Group is composed of dark-green and grey siltstone, and shale with minor sandstone and locally abundant limestone nodules (Strong *et al.*, 1978; Figure 2). It formed in a shallow-marine, possibly intertidal environment

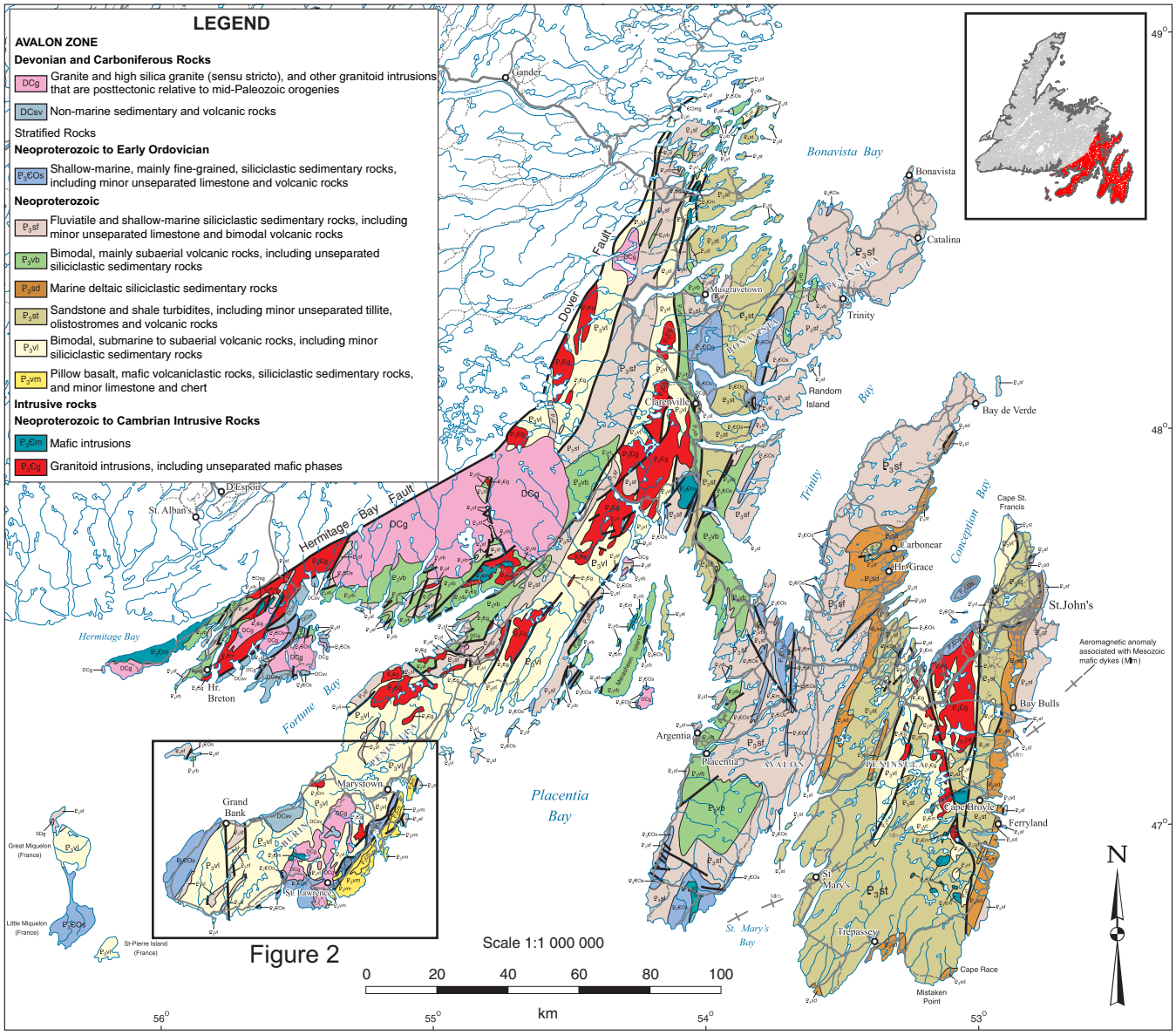

Figure 1. *Simplified geological map of the Avalon Zone (after Colman-Sadd* et al.*, 1990).*

in a Cambrian stable platform (van Staal *et al.*, 1998; Fortey and Cocks, 2003; Hamilton and Murphy, 2004). The sedimentary rocks hosting the fluorite mineralization in the AGS area are interpreted to be part of the Inlet Group (Strong *et al.*, 1978), although recently Evans and Vatcher (2009) suggested that these rocks are part of the Marystown Group based on the degree and style of deformation they exhibit.

The Rocky Ridge Formation (RRF) occurs as a discontinuous sequence of riebeckite-bearing felsic volcanic rocks in the SLG (Strong *et al.*, 1978; Figure 2). It consists of rhyolite flows, ignimbrite, agglomerate and tuffs. The mineralogy of the RRF is similar to the mineralogy of the SLG, and it is interpreted as a volcanic equivalent of the granite.

The Clancey's Pond Complex is composed of ignimbrites and pyroclastic breccia (Strong *et al.*, 1978; Figure 2). It occurs in the vicinity of the Grand Beach complex and is interpreted as the volcanic equivalent of the porphyry, which has a chemical affinity to the SLG.

The intrusive rocks include the Mount Margaret gabbro, Loughlins Hill Gabbro, Seal Cove gabbro, Anchor Drogue granodiorite, Grand Beach complex and the SLG (Strong *et al.*, 1978; Figure 2). The age of most of the intrusions is uncertain. The Grand Beach complex yielded an age of 394 +6/-4 Ma (Krogh *et al.*, 1988; Kerr *et al.*, 1993b). The SLG is genetically and spatially associated with fluorite mineralization and is described in more detail below.

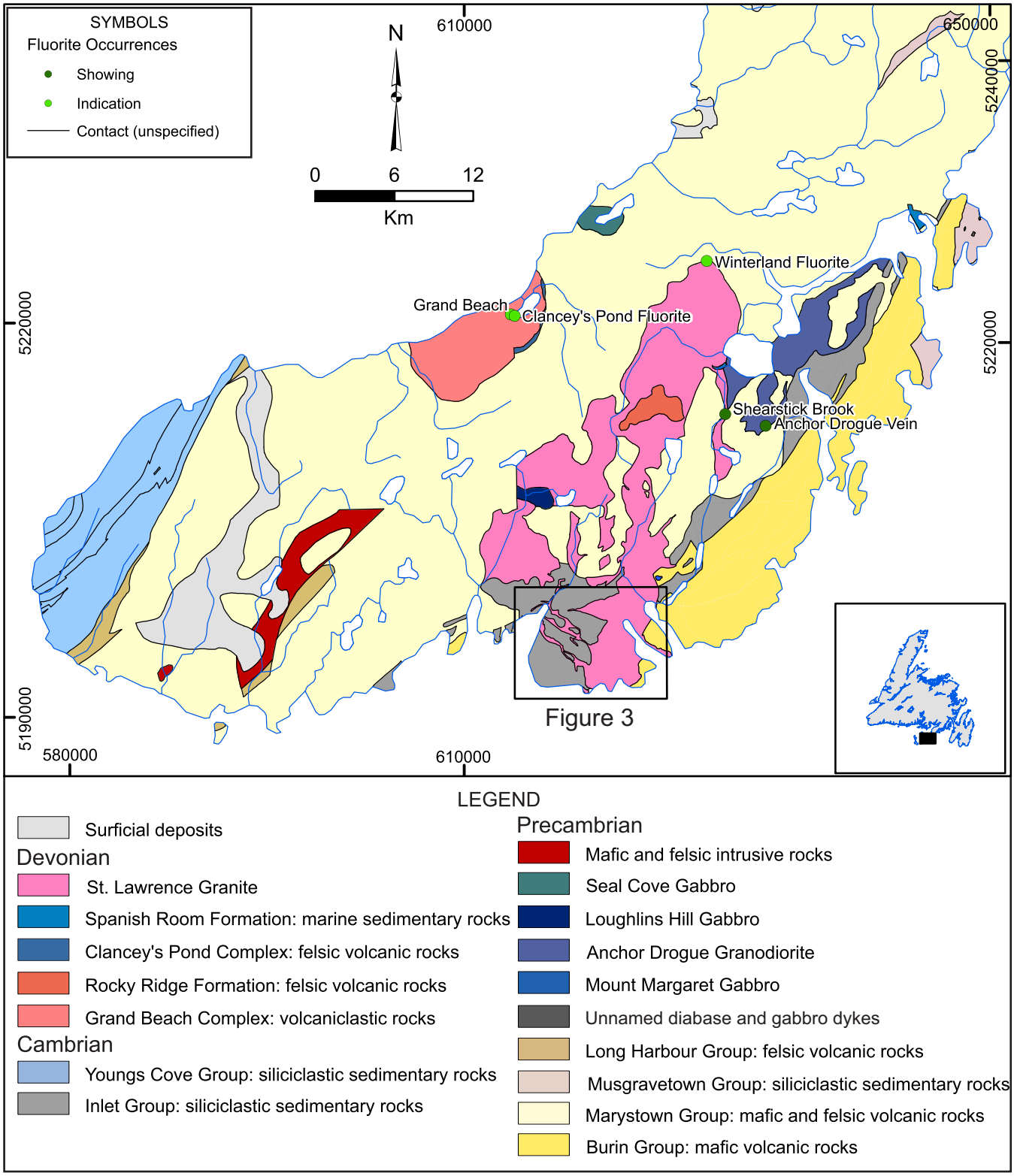

Figure 2. *Geology of the St. Lawrence area (after O'Brien* et al.*, 1977 and Strong* et al.*, 1978).*

Nine rock types have been described as occurring in dykes. In decreasing order of abundance, they are hornblende diorite, gabbro, coarse diabase, fine diabase, felsite, quartz–feldspar porphyry, trachybasalt, trachyandesite and granite (Wilton, 1976; Strong *et al.*, 1978). The dykes are most abundant in the Burin Group.

The St. Lawrence area was affected by thrusting and associated folding observed in the Marystown Group and Inlet Group (Strong *et al.*, 1976). The thrust faults strike northeasterly with a northwesterly dip around 45°. Thrust faulting occurred prior to the intrusion of the SLG and indicates a period of regional compression. Thrust faulting and associated folding are intersected by later normal faults striking around 10° and indicating regional extension (Williamson, 1956; Teng, 1974).

ST. LAWRENCE GRANITE

The SLG is a north-trending intrusion outcropping over an approximate area of 30 by 6 km (Teng, 1974; Figure 2). It intruded along pre-existing normal faults that influenced the northerly elongated shape of the granite in a direction of 10°. Teng (1974) described four phases of the granite including coarse-grained granite, medium-grained granite, fine-grained granite and porphyritic granite. The contacts between the different phases are sharp. Tuffisites, consisting of fragments of granite in a fine-grained material of similar composition, are common. Quartz–feldspar porphyritic (rhyolite porphyry) sills occur to the west of the SLG, specifically in the AGS area, as noted by both Van Alstine (1948) and Teng (1974). The sills generally dip gently to moderately to the north.

The SLG is composed of quartz, orthoclase and albite and minor amounts of riebeckite, aegirine, biotite, fluorite, magnetite and hematite (Teng, 1974). Chlorite occurs as an alteration from mafic minerals. The rhyolite porphyry consists of the same minerals and has a porphyritic texture, where the phenocrysts are euhedral quartz, orthoclase and minor plagioclase.

The SLG is interpreted to have been intruded at shallow depth based on the presence of extensive dyke swarms of rhyolite porphyries, preserved portions of a volcanic cover sequence (Rocky Ridge Formation), miarolitic cavities, gas breccias (tuffisites), and vuggy pegmatitic segregations indicative of volatile exsolution (Van Alstine, 1948; Strong *et al.*, 1978; Kerr *et al.*, 1993a, b). Around St. Lawrence, it is interpreted to represent the roof of the pluton, suggested by the abundance of porphyritic phases and fluorite veins (Williamson, 1956; Kerr *et al.*, 1993a), and likely plunged to the north at a relatively shallow angle.

A Rb–Sr age of 334 ± 5 Ma (Bell *et al.*, 1977) was recalculated by Kerr *et al.* (1993b) to 315 Ma. However, the most recent, and likely the more accurate, dating of the intrusion yielded an age of 374 ± 2 Ma (U–Pb in zircon, Kerr *et al.*, 1993b). The rhyolite in the AGS area was dated in this study and yielded an age of 377.2 ± 1.3 Ma (*see* below; Figure 4).

Major-element chemistry suggests that the SLG is an alkali-feldspar granite, being peralkaline to metaluminous, ferroan in composition and having a high SiO_2 content (Kerr *et al.*, 1993a). The trace-element compositions indicate that it is highly fractionated (depleted in Sr, Ba, Eu) and plots as a 'within-plate granite' (A-type). It has a very high volatile content, including fluorine (average 1308 ppm, Teng, 1974). According to Kerr *et al.* (1993a), it originated from the melting of a feldspar-rich source (or possibly a hornblende-bearing source material from the lower crust) with progressive melting of feldspars, represented first by plagioclase, and then K-feldspar (suggested by the Ba depletion). The high fluorine is postulated to have originated from fluorine being trapped in hornblende (Van Alstine, 1976).

The SLG is one of the many Devonian postorogenic granites that intruded the Avalon and Gander zones (Kerr *et al.*, 1993a). The source of these intrusions is mantle-derived magmas of mafic or intermediate composition that interacted with various components of the continental crust. As suggested by Nd-isotope geochemistry, the continental crust in the eastern Avalon region was more juvenile in character than elsewhere in eastern Newfoundland (Kerr *et al.*, 1993a).

ST. LAWRENCE FLUORITE DEPOSITS

The fluorite deposits in St. Lawrence have been the focus of many studies including those of Van Alstine (1948, 1976), Williamson (1956), Teng (1974), Teng and Strong (1976), Strong *et al.* (1978, 1984), Richardson and Holland (1979), Strong (1982), Collins (1984, 1992), Collins and Strong (1988), Irving and Strong (1985), Gagnon *et al.* (2003), Kawasaki and Symons (2008), Kawasaki (2011), Sparkes and Reeves (2015), Reeves *et al.* (2016) and Magyarosi (2018). The following is a summary from those studies.

Fluorite mineralization associated with the SLG formed as open-space fillings in tension fractures created by regional stresses and contraction resulting from the cooling of the granite. Fluorine-rich volatiles separated from the cooling granite, and escaped along structures to be subsequently deposited in fractures in the upper part of the granite. Repeated movement along fractures resulted in the brecciation of host rocks and pre-existing vein material, thus creating space for several successive phases of fluorite mineral-

ization. Volatiles generally did not escape into the host sedimentary rocks due to the impermeability of the hornfelsed sediments overlying the granite (Teng, 1974; Strong, 1982). As such, most of the fluorite veins are hosted in the granite. Further, the lack of fluorite veins in the country rocks may be due to open fissures, formed as a result of cooling in the granite, narrowing and closing as they passed from the granite into the country rocks that were not subjected to cooling and contraction (Williamson, 1956). The AGS vein system is an exception, being hosted mainly in sedimentary rocks and rhyolite sills intruding the sediments. The fluorite veins are epithermal, suggested by low temperature and pressure assemblages, vuggy veins, abundance of breccia, and colloform and crustiform structures.

Strong *et al.* (1984) and Collins (1992) completed detailed analysis of fluorite samples from several veins and concluded that the main control on fluorite deposition was an increasing pH caused by the boiling of magmatic fluids. Fluid-inclusion studies suggest that the fluorite formed between temperature ranges of 100 and 500°C, with both increasing and decreasing temperatures observed during crystal growth. Formation pressures were between 65 and 650 bars. Additional fluid-inclusion studies from this study have focused on the AGS deposit (*see* below). Oxygen isotopes suggest mixing of magmatic fluids with cool meteoric fluid. Rare-earth element (REE) concentrations in the different ore zones and textural types of fluorite indicate a magmatic origin (Strong *et al.*, 1984).

There are more than 40 fluorite veins in the St. Lawrence area, ranging in size from a few cm to 30 m in width and up to 3 km in length (Figures 2 and 3). Tension fractures perpendicular to the normal fault (~100°), along

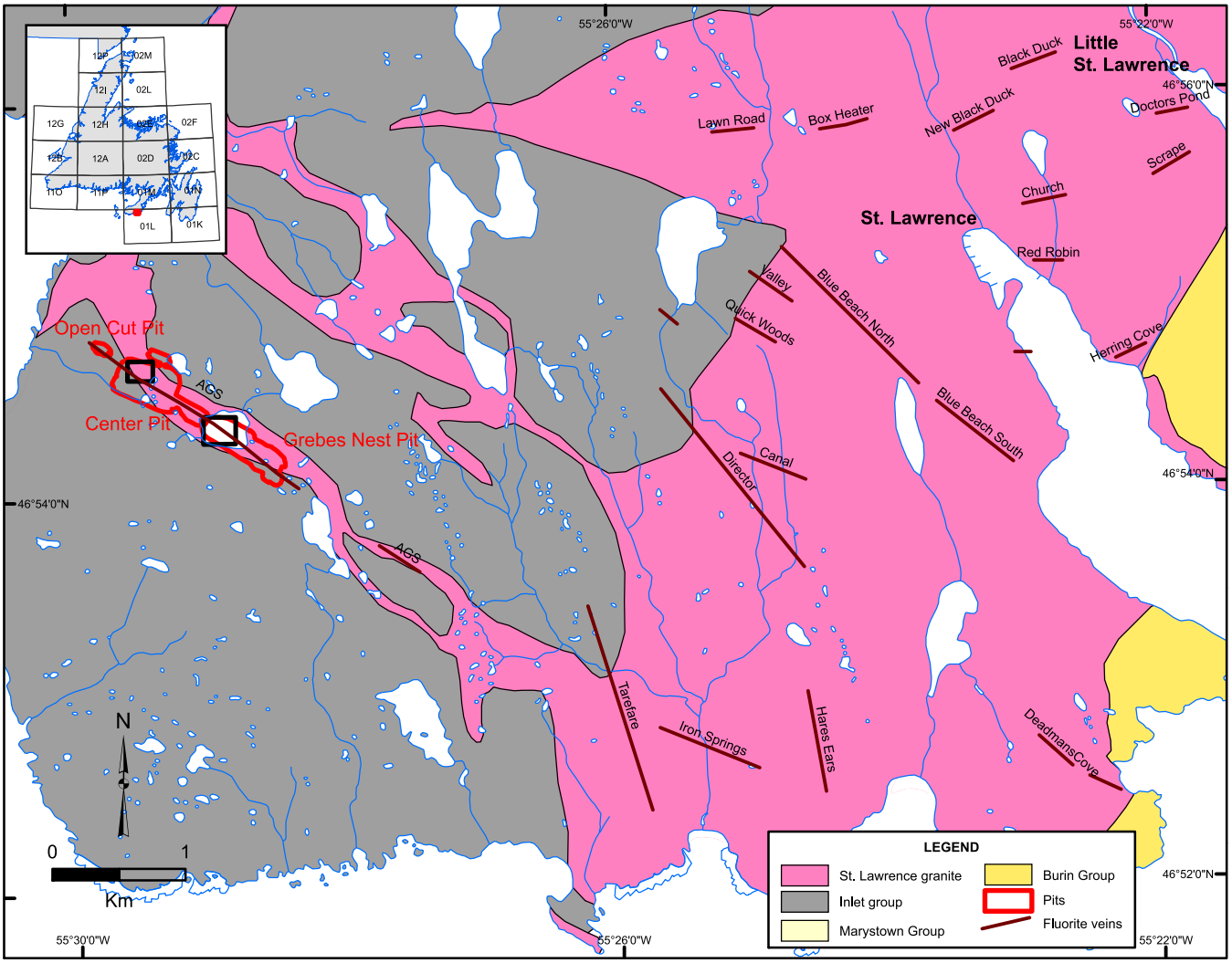

Figure 3. *Main fluorite occurrences in the St. Lawrence area (modified after Strong* et al.*, 1976, 1978 and Wilson, 2000). Black rectangles show locations of detailed maps in Figures 10 and 11.*

which the SLG intruded, and associated shear structures (~60 and 140°) controlled the orientation of the fluorite veins. There are variations in thickness along strike and with depth. Four major types of fluorite veins are described:

1. North–south-trending low-grade veins (Tarefare, Director, Hares Ears, Blue Beach North and South);

2. East–west-trending high-grade veins (Black Duck, Lord and Lady Gulch, Iron Springs, Canal);

3. Northwest–southeast-trending veins in sedimentary rocks containing high-grade and low-grade mineralization (AGS); and

4. East–west-trending peripheral veins containing significant amounts of barite with fluorite (Meadow Woods, Lunch Pond, Clam Pond, Anchor Drogue).

In addition to the differences in the orientation and grade between the major types of fluorite veins, Van Alstine (1948), Williamson (1956), Wilson (2000) and Reeves et al. (2016) also noted the abundance of green fluorite and increased amount of sulphide minerals in the peripheral veins and veins not hosted in granite compared to the granite-hosted veins.

AGS Deposit

The AGS vein system, as currently defined, is approximately 1.85 km long and consists of several fluorite veins running almost parallel to each other, with local pinching and swelling observed (Sparkes and Reeves, 2015; Reeves *et al.*, 2016; Figure 3). The veins are in sedimentary rocks, as well as in rhyolite sills that intrude the sediments and dip gently to the north. The sedimentary rocks are dark-grey to green shales of the Inlet Group. The SLG is intersected in deeper holes between 250 and 300 m and drilling has confirmed the continuation of the deposit well into the SLG.

The veins are fault-controlled and range in width from less than 2 m to up to 30 m. The strike length of major veins is between 400 and 700 m. The three major veins include the North, South and Grebes Nest Pit (GP) veins. The fluorite resource in the AGS vein system has been calculated by CFI to be 9 389 049 tonnes at 32.88% fluorite (NI 43-101 compliant, Sparkes and Reeves, 2015).

U–Pb GEOCHRONOLOGY

ANALYTICAL METHODS

One rhyolite sample from the western part of the AGS area was selected for age dating. The sample was processed using standard techniques of crushing and concentration of a heavy mineral separate, and zircon was prepared as described in Sparkes and Dunning (2014). All zircon was chemically abraded (*cf.* Mattinson, 2005) prior to final selection of crystals for dissolution and analysis. Three fractions of either 2 or 3 crystals were dissolved and their lead and uranium purified. Lead and U isotopic ratios were measured using thermal ionization mass spectrometry by peak jumping on an ion-counting secondary electron multiplier, and final isotopic ratios were calculated using in-house software.

RESULTS

The zircon crystals from the sample are small, euhedral, and appear to be a simple igneous population (Plate 1). In cathodoluminescence (CL), the few imaged crystals display intergrown crystals, unidentified inclusions in their cores, and one shows a possible high U core with damage and cracks (Plate 2). These show less variation in CL intensity than is usual in zircon. Geochronology of the rhyolite yielded a weighted average $^{206}Pb/^{238}U$ age of 377.2 ± 1.3 Ma (Figure 4; 95% confidence interval, mean square weighted

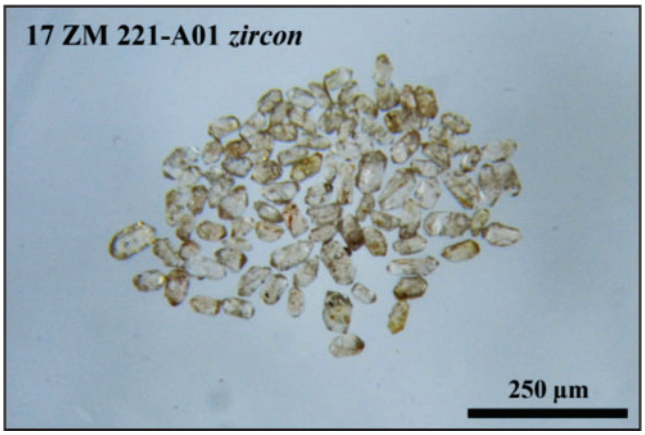

Plate 1. *Photo of zircons from rhyolite used for geochronology.*

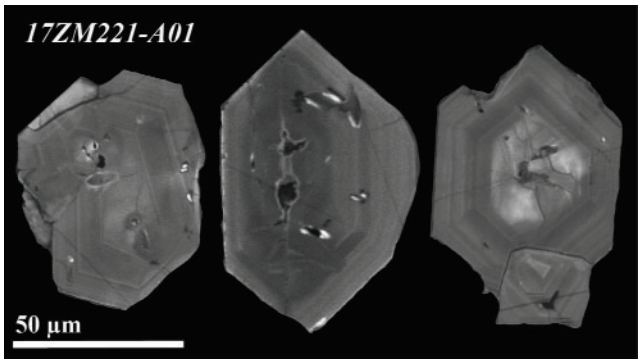

Plate 2. *CL image of zircons.*

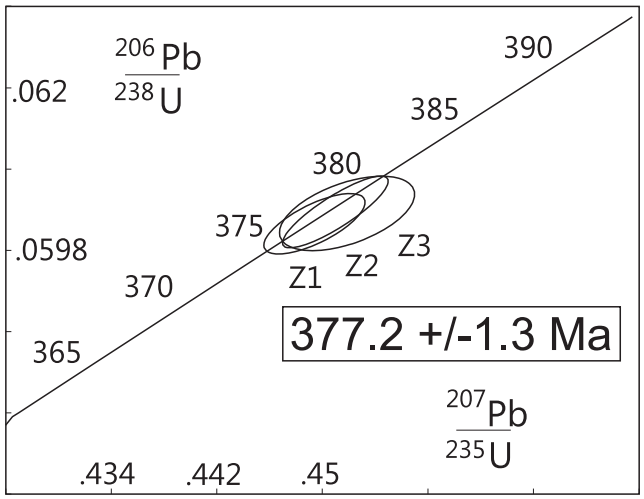

Figure 4. *U–Pb Concordia diagram for the rhyolite.*

deviation (MSWD) = 0.23), suggesting that the rhyolite sills are slightly older than the granite, which was dated at 374 ± 2 Ma (Kerr *et al.*, 1993b). The AGS area is underlain by the SLG, but no field relationships have been observed between the rhyolite and the SLG. However, similarities in the mineralogy and major-, minor- and trace-element geochemistry of the rhyolite and the SLG suggest that the rhyolite is an earlier phase of the SLG.

Rhyolite Sills

The rhyolite sills have a porphyritic texture and are composed of quartz and feldspar (orthoclase and minor plagioclase) phenocrysts in a groundmass of the same minerals. Other phases include minor chlorite (alteration of biotite, amphibole and pyroxene); sericite (alteration of feldspars); and trace amounts of zircon, rutile and several REE minerals including monazite, xenotime and thorite. Zircon, rutile, REE minerals, hematite and locally fluorite are spatially associated with chlorite (Plates 3A, B and 4) and occur interstitially to the other minerals and/or in miarolitic cavities, suggesting that they were the last to crystallize; a feature common to peralkaline granites (Clemens *et al.*, 1986; Sallet *et al.*, 2000; Agangi *et al.*, 2010).

The presence of the same minerals forming the phenocrysts and the groundmass in the rhyolite sills indicates two-stage cooling, with strong undercooling in the second stage. The rhyolite likely separated early during ascent of the granitic magma, potentially because of a sudden pressure drop, and intruded at shallower levels, while still partially molten. There, the rhyolite subsequently cooled faster than the main body of the SLG as suggested by abundant textural evidence for undercooling, such as abundant granophyric texture and skeletal, dendritic, fine-grained K-

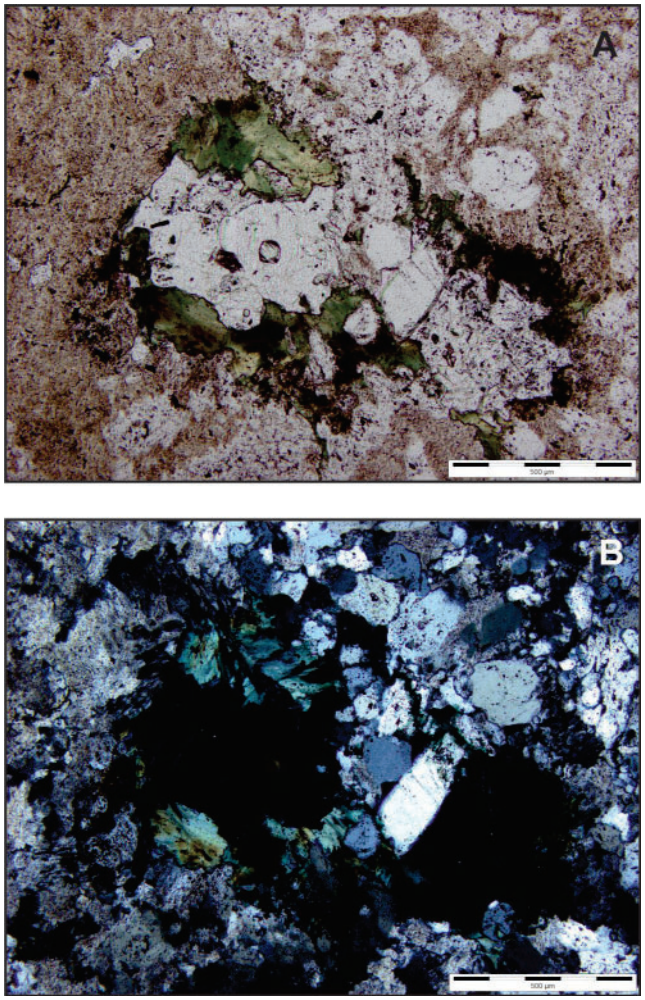

Plate 3. *A) Chlorite (green), quartz (white, clear), fluorite (white, rough) in plane-polarized light; B) Same as A under crossed polars.*

feldspar surrounding the quartz phenocrysts (Plate 5A, B; Candela, 1997).

Samples of the SLG, including the rhyolite sill, returned values of SiO_2 between 75.36 and 83.06 wt. % (average of 77.10), Al_2O_3 between 7.83 and 11.92 wt. % (average 10.68), Fe_2O_3 between 1.47 and 2.99 wt. % (average 2.23), CaO between 0.06 and 0.58 wt. % (average of 0.30), Na_2O between 2.11 and 4.19 wt. % (average of 3.28) and K_2O between 3.55 and 5.41 wt. % (average 4.69). The average F content is 1229 ppm with a range between 255 and 2468 ppm. It is an A-type or within-plate granite (Figures 5 and 6; Loiselle and Wones, 1979; Pearce *et al.*, 1984; Whalen *et al.*, 1987), which is consistent with the conclusions of Kerr *et al.* (1993a). Based on major-element chemistry, the SLG is ferroan, alkalic to calc-alkalic and peralkaline (Figure 7; Shand, 1922; Frost *et al.*, 2001; Frost and Frost, 2008). The

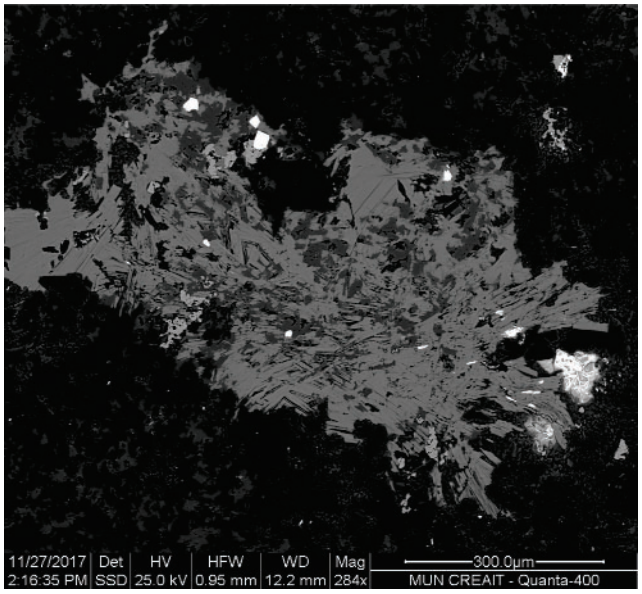

Plate 4. *SEM image of chlorite (light grey, fibrous), zircon (white, euhedral) and monazite (white, subhedral).*

SLG is enriched in all REE's (except Eu) and some of the trace elements (Rb, U, Th) relative to chondrites and primitive mantle (Figures 8 and 9). The light-REE's are more strongly enriched with a negative slope from La to Sm, whereas the heavy-REE's are represented as a flat line segment. Negative Ba, Sr, P, Ti and Eu anomalies characterize the SLG and the rhyolite (Figure 9).

STRUCTURE OF THE DEPOSIT

Detailed mapping of the western part of the GP veins and the North Vein in the Center Pit are illustrated in Figures 10 and 11, respectively. Structural measurements were also obtained from the Open Cut Vein and the eastern part of the Grebes Nest Pit. Overall, the strike of the main GP veins ranges between 93 and 165º with an average of 124º and the orientation of the North Vein ranges between 95 and 142º with an average of 117.5º (Figure 12). There are several minor veins, especially in the Grebes Nest Pit, that are oblique to the main vein. The veins typically dip steeply between 55 and 90º to the southwest, whereas a few veins are steeply dipping between 60 and 90º to the northeast.

The orientation of the AGS veins differs from the main granite-hosted veins (Tarefare, Director and Blue Beach), which have orientations ranging between 135 and 160º (Figure 3). The orientation of the main granite-hosted veins is controlled by the direction of maximum shears (~60 and ~140º) developed following the intrusion of the granite as a result of regional stresses (Williamson, 1956; Teng, 1974). The reason for the difference in the orientation of the AGS veins has not been investigated, but it is likely that the struc-

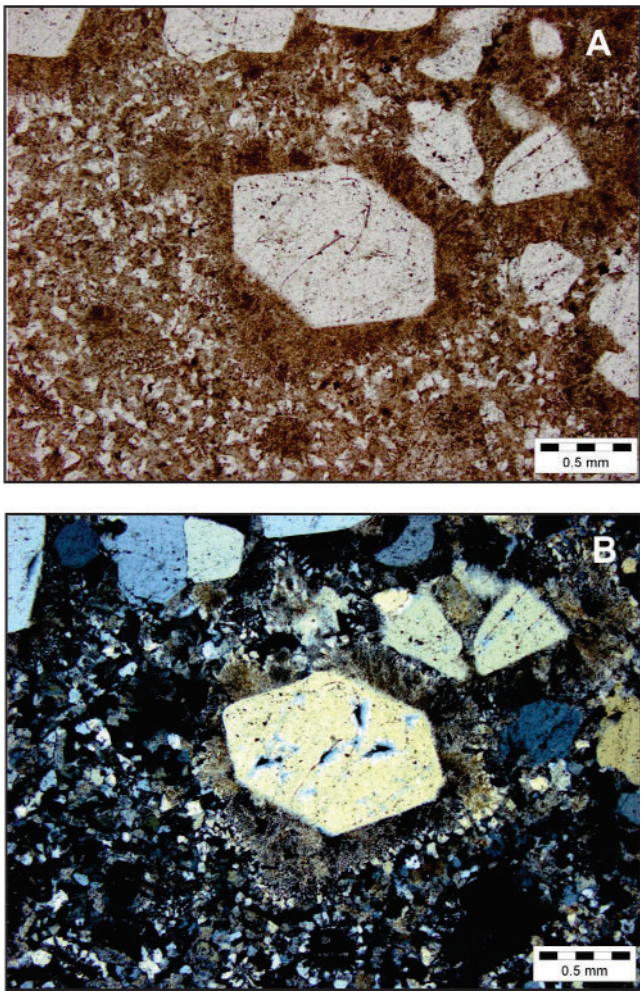

Plate 5. *A) Dendritic feldspar surrounding euhedral quartz phenocryst in plane-polarized light, B) Same as A under crossed polars.*

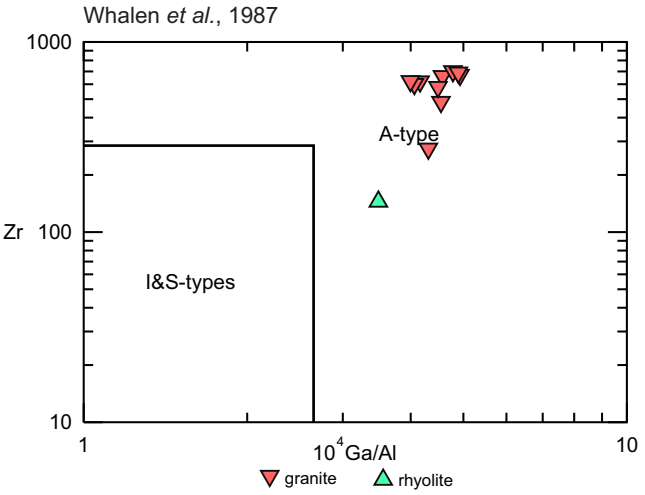

Figure 5. *Zr* vs. *Ga/Al classification of the SLG (Whalen* et al.*, 1987).*

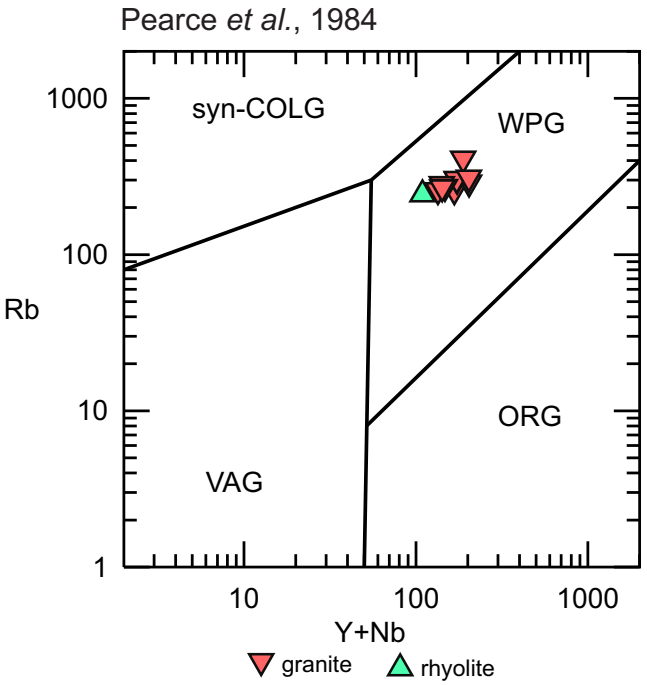

Figure 6. *Rb* vs. *Y+Nb classification of the SLG (Pearce* et al.*, 1984).*

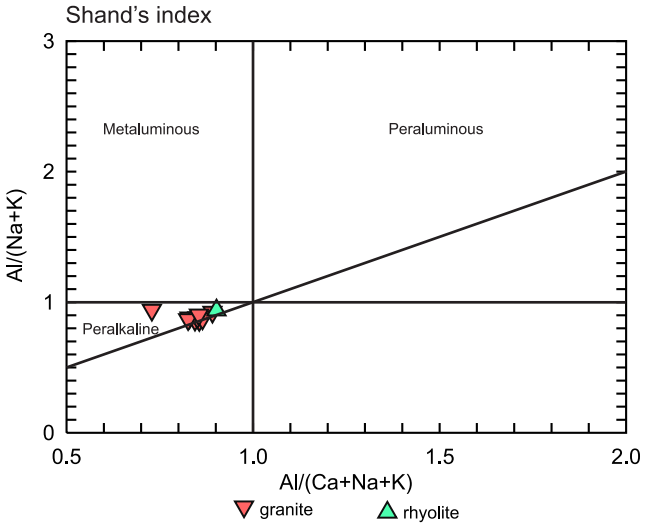

Figure 7. *Shand's index plot of the SLG (Shand, 1922).*

ture controlling the AGS veins existed before the intrusion of the SLG, possibly during earlier thrust faulting, and was reactivated around the time of the intrusion. The lack of ponding of mineralizing fluids, typically described at other SLG-sediment contacts (Strong, 1982), also suggests the presence of a structure that allowed the mineralizing fluids to escape into the sedimentary rocks.

The fluorite veins in the AGS deposit are controlled by a sinistral strike-slip fault. Faulted contacts of barren or min-

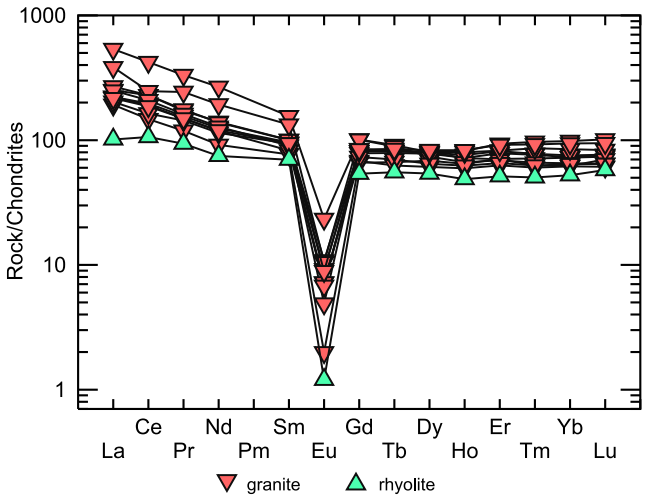

Figure 8. *REE element distribution of the SLG normalized to chondrites (Sun and McDonough, 1989).*

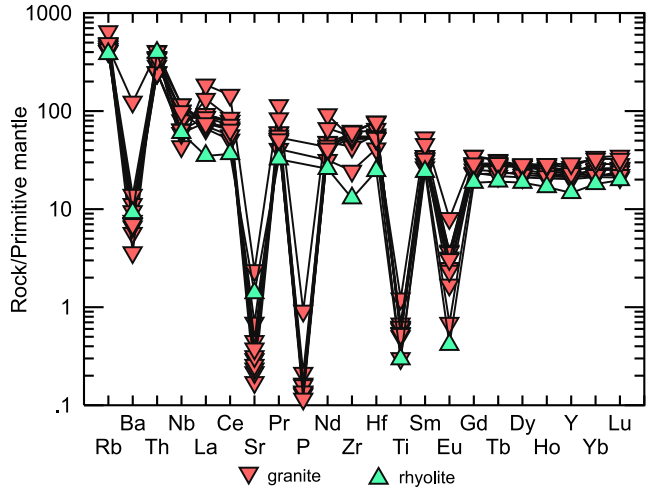

Figure 9. *Trace-element distribution of the SLG normalized to primitive mantle (Sun and McDonough, 1989).*

eralized rhyolite and sediment are present throughout the deposit (Plate 6). The presence of extensive hydrothermal breccia indicates that the fault was brittle with high fluid pressure (Sibson, 1977; Nicolas, 1987), caused by fluids escaping from the cooling granite and rhyolite sills underneath. Movement along the fault resulted in brecciation of the host rocks and by the influx of fluids that precipitated hydrothermal minerals, including fluorite, and sealed the cracks; this process repeated itself until the fault became inactive. Earlier phases of mineralization were broken up and cemented by subsequent phases. This is similar to other fluorite veins in the St. Lawrence area (Van Alstine, 1948; Teng and Strong, 1976; Strong *et al.*, 1984) and is described as the "fault-valve model" by Sibson *et al.* (1988). Vugs and comb textures developed in some phases suggest that at least

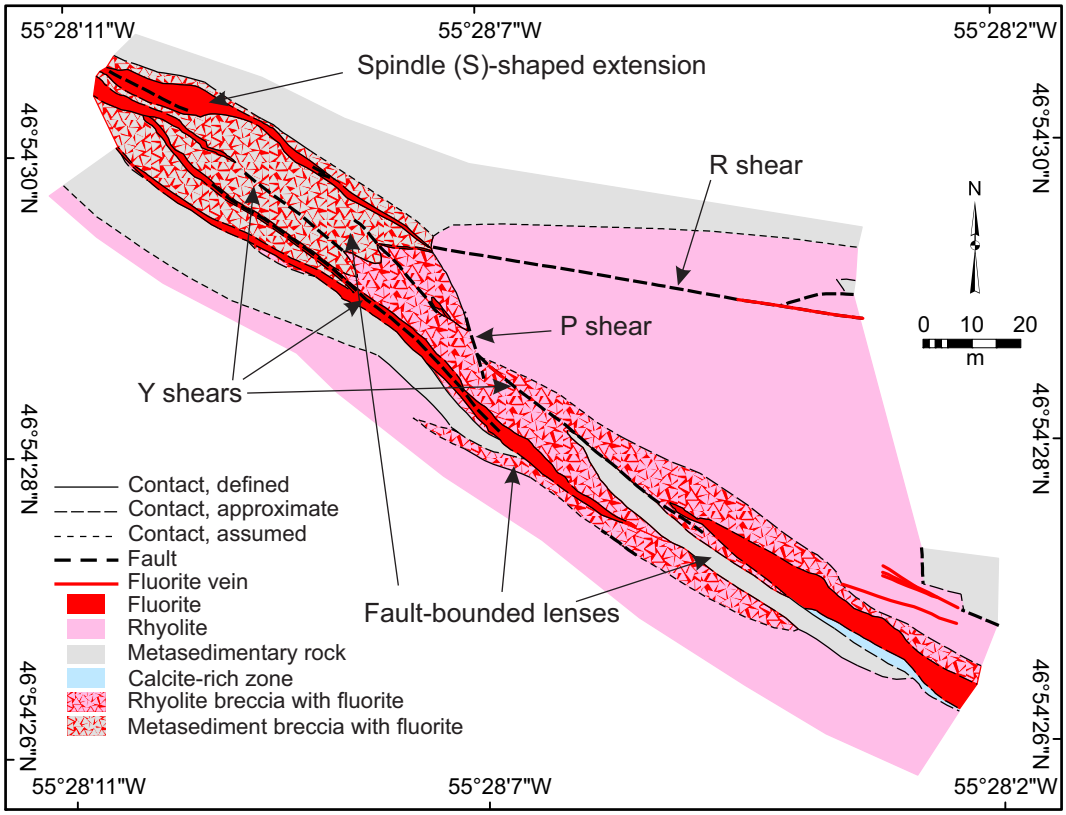

Figure 10. *Detailed map of the GP veins in the Grebes Nest Pit.*

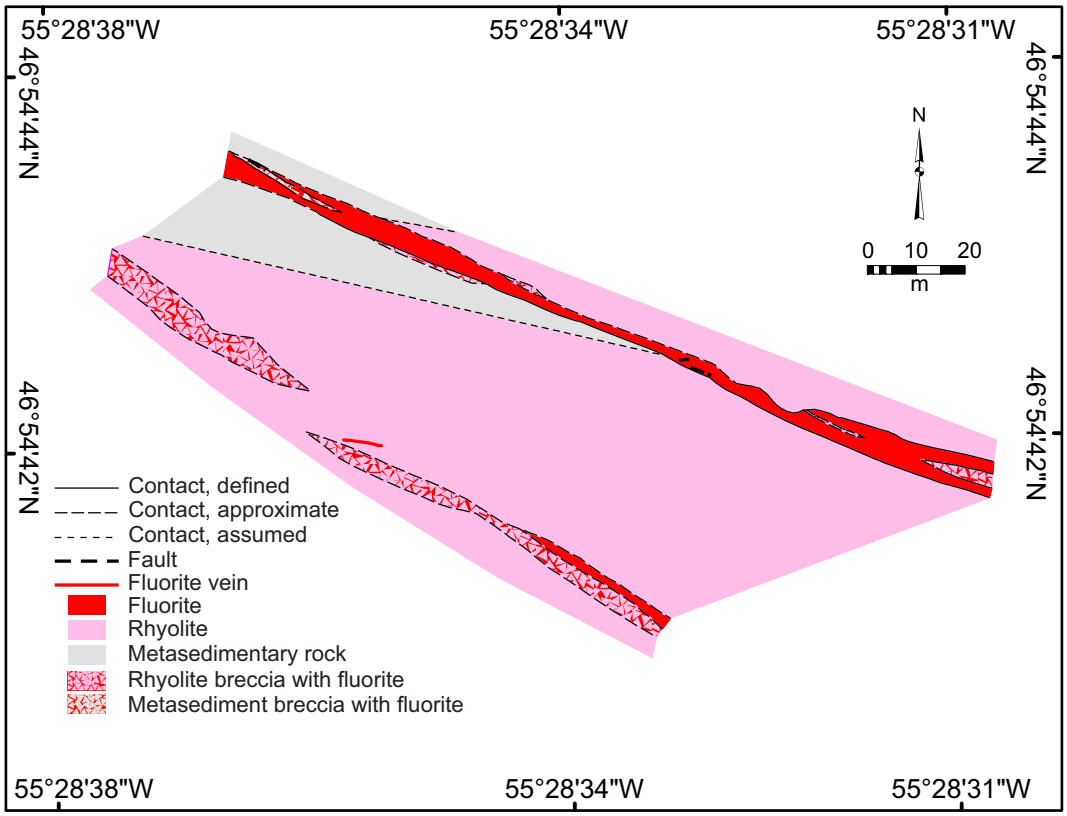

Figure 11. *Detailed map of the North Vein in the Center Pit.*

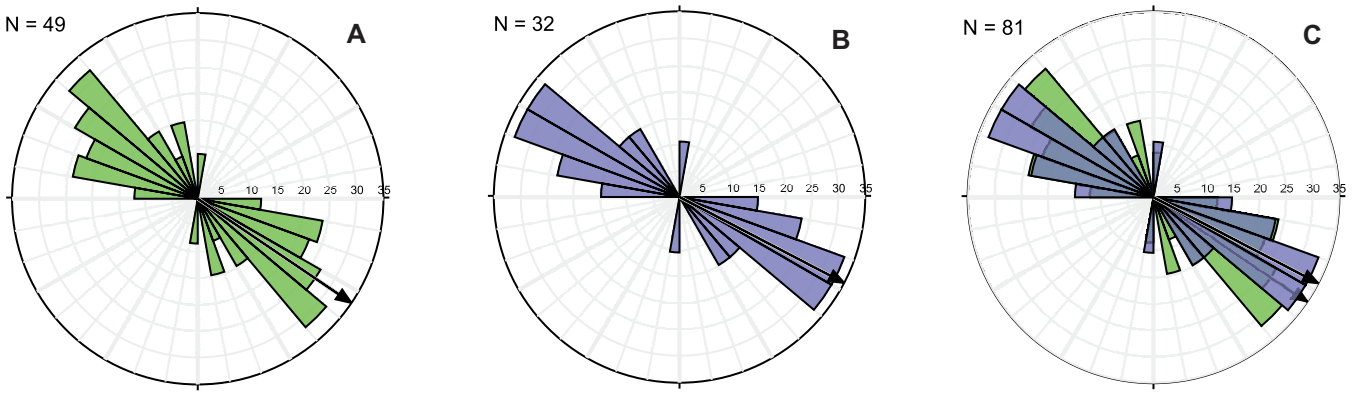

Figure 12. *Stereonet projections of vein contacts in the Grebes Nest Pit (A), in the North Vein (B), Center Pit and both veins (C) (using Stereonet 10.0, Allmendinger* et al.*, 2012; Cardozo and Allmendinger, 2013).*

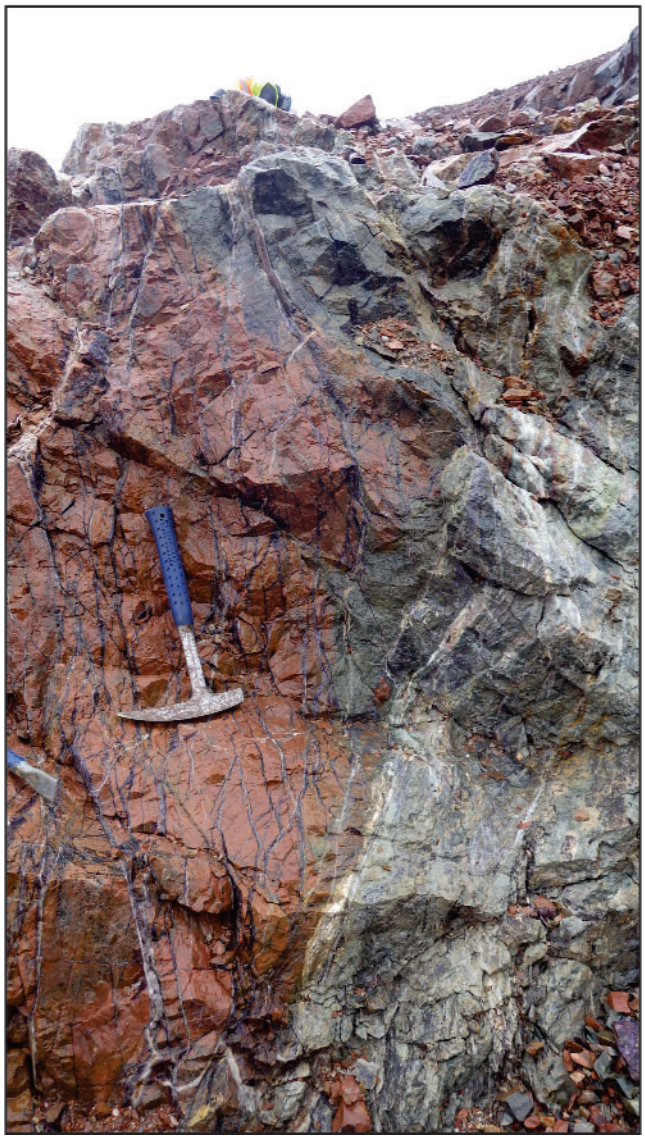

Plate 6. *Faulted contact of the sediment and rhyolite with fluorite in both units.*

some of the veins were dilatational (Plates 7 and 8), indicating that there were local extensional areas developed along the main strike-slip fault. This is especially obvious in the northwestern end of the Grebes Nest Pit, where the high-grade, grey fluorite forms elongated crystals up to 20 cm in length, perpendicular to the walls of the vein or breccia clasts of earlier vein material. Sparkes and Reeves (2015) also observed that fluorspar deposited in the main phases (phases 4, 5 and 6; *see* below and Table 1) is volumetrically significant and occurs during a period of prolonged dilation.

The GP veins are composed of fault-bounded lenses of wallrocks and earlier phases of fluorite mineralization (Figure 10). Nearly horizontal (5 to 10°) slickensides plunging southeast are observed on fault surfaces (Plate 9). Sinistral movement is indicated by the slickenside steps developed on fault surfaces, the orientation of sigmoidal tension gashes filled with purple fluorite in rhyolite and sediment clasts (Plate 10), the left-lateral displacement of earlier veins (Plate 11) and the direction of oblique faults throughout the deposit (Riedel (R) shears, Figure 10). Despite the brittle nature of the fault, drag folding of earlier, chlorite-rich shears in brecciated rhyolite is locally observed and also indicates sinistral movement (Plate 12).

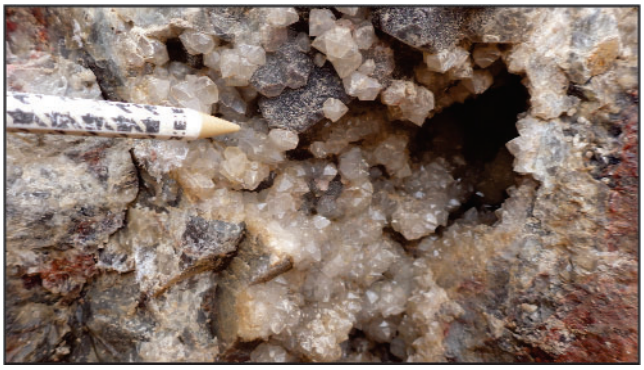

Plate 7. *Vug with late quartz crystals on top of cubic fluorite.*

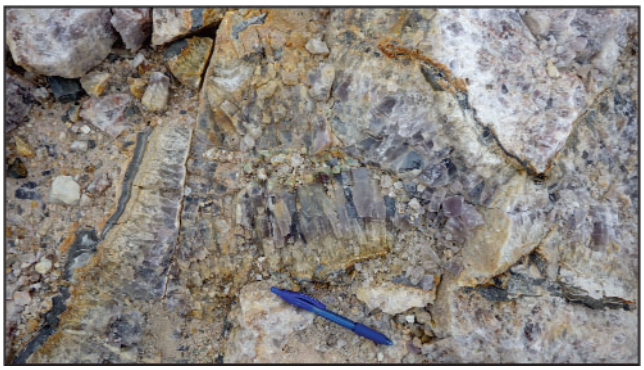

Plate 8. *Comb-textured grey fluorite in the Grebes Nest Pit.*

Plate 9. *Horizontal slickensides.*

Plate 10. *Sigmoidal tension gashes in rhyolite clast indicating sinistral movement.*

Plate 11. *Sinistral displacement of earlier fluorite veins in rhyolite.*

The features of the GP veins suggest that the structure controlling the mineralization is a well-developed strike-slip fault. The first structures that appear in a strike-slip fault are the Riedel shears (R shears), which are oblique to the main shear direction (Figures 10 and 13; Naylor *et al.*, 1986; Dooley and Schreurs, 2012 and references therein). The exact orientation of the R shears depends on the rock type and the amount of fluids (Dooley and Schreurs, 2012). With increasing movement, the R shears further spread along strike and swing in the direction of the main movement. At the same time, P shears develop and cross the direction of the main movement in the opposite direction at a slightly lower angle. With further movement, the R and P shears are linked together to form a zone consisting of a series of fault-bounded shear lenses that are composed of wallrocks and earlier vein material. Most of the movement is taken up by a central Y shear parallel to the main shear direction. With continued movement new R and P shears develop.

Plate 12. *Drag folds of earlier chlorite-rich shears in brecciated rhyolite.*

The evolution of the strike-slip fault is consistent with the paragenetic sequence of hydrothermal events (*see* below). The fault-bounded lenses are composed of barren and weakly to moderately mineralized wallrocks containing purple fluorite stockwork and hydrothermal breccia, representing early stages of hydrothermal activity. Some of the faults separating the lenses host veins containing yellow, grey, green and blue fluorite, that all formed after purple fluorite. Most of the high-grade mineralization in the GP veins is hosted in a major S-shaped extension zone that developed late in the evolution of the fault. This extension zone starts at the contact of rhyolite and sediment, suggesting that the location of extension zones were probably controlled by lithological contacts between the two rock types. The oblique veins, controlled by the youngest R shears, are typically composed of green and blue fluorite representing the last stage of mineralization.

The direction of the North Vein (117.5º average) is slightly different from the GP veins and it is composed of very high-grade fluorite (Figure 11). Horizontal slickensides indicating sinistral movement are also observed in the North Vein, but the textures and phases of fluorite indicate significant early extension associated with this vein. Barren breccia and purple fluorite are typically followed by the reddish grey and elongated grey fluorite. Green fluorite crystallized after the grey fluorite. Vugs up to 1 m in length are filled with clear and blue cubic fluorite up to 6 cm in length along with late quartz (Plate 7).

PARAGENETIC SEQUENCE

Mineralization in the AGS deposit is divided into early, main and late stages. A more detailed paragenetic sequence is shown in Table 1. The samples reported herein were collected for this research project and the grades of the individual phases below do not represent the highest grades in the deposit. The amount of fluorite (CaF_2) in the collected samples was calculated from the fluorine (F) amount measured

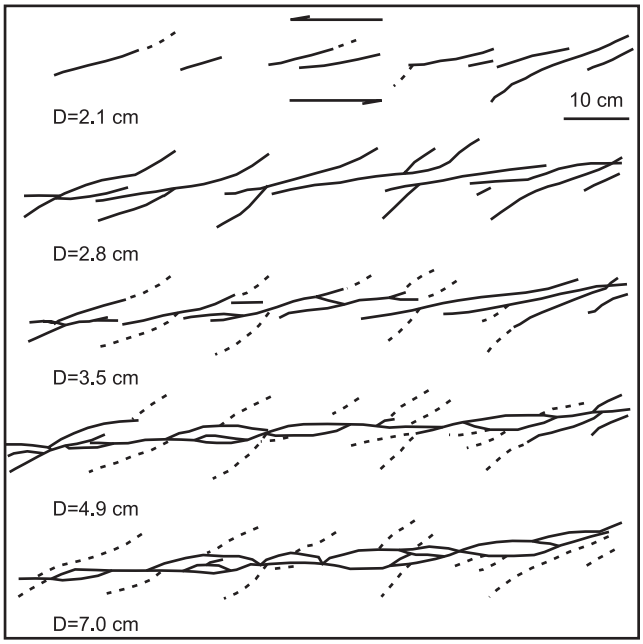

Figure 13. *Evolution of a strike-slip fault based on experiments (adapted from Naylor* et al.*, 1986).*

in the laboratory taking into account the mass percent of F (48.666%) in the molar mass of CaF_2 (78.074 g/mol).

Fluorite is the main mineral in the veins and occurs in purple, yellow, green, blue, grey, white, red, pink and tan colours. The pink and tan occur in fine-grained, banded fluorite ore and the colour is due to the presence of fine-grained hematite. Purple fluorite varies between fine or coarse grained, whereas the other coloured fluorites are typically coarse to very coarse grained. Most of the fluorite is cubic, but the green fluorite is octahedral. Purple fluorite has been observed as cube octahedrons (cubes with octahedral faces cutting off the corners of the cube).

The fluorite in all phases exhibits a variety of textures including hydrothermal breccia, stockwork veins, massive, crustiform, colloform, cockade, comb and zonal crystals. Breccia and stockwork veins are typical in the early stage. Colloform banding is more common in the last phase of the early stage (fine-grained, banded fluorite), but occurs throughout the other phases. Cockade, massive and comb textures are typical in the main stage of mineralization.

Calcite is locally abundant and occurs in variable amounts in every phase in the AGS deposit, but particularly in the High Carbonate Zone, located in the centre of the Grebes Nest Pit (Sparkes and Reeves, 2015), where the amount of calcite in the veins may locally reach 50% or more. Quartz is typically associated with both the earlier phases of hydrothermal activity (barren breccia, purple flu-

Table 1. Paragenetic sequence of hydrothermal events in the AGS area

Stage	Phase		Description
Early stage	1	Brecciation of host rocks	Brecciated, weakly to strongly altered sedimentary rocks and rhyolite in a quartz-rich matrix.
	2	Purple fluorite stockwork and/or	Purple fluorite and quartz forming stockwork veins and hydrothermal breccia with clasts of host rocks.*
	3a	Banded, fine-grained fluorite and/or yellow, coarse-grained fluorite	Finely banded, fine-grained fluorite and/or coarse-grained yellow fluorite.
	3b	Hematite–fluorite–quartz	Hematite with quartz and fluorite.
Main stage	4	Reddish grey fluorite	Massive, coarse-grained, grey, transparent fluorite, locally slightly reddish or pink.
	5	Fine-grained banded sulphides	Composed of sphalerite and galena.
	6	Grey elongated fluorite	Massive, grey fluorite with elongated crystals up to 20 cm in length.
Late stage	7	Green, blue and white, coarse-grained fluorite	Alternating layers of coarse-grained green, blue and white fluorite with disseminated sphalerite and galena.
	8	Clear or blue, cubic fluorite	Clear or blue cubic fluorite up to 6 cm along edges occurs filling vugs.
	9a	Blastonite	Breccia composed of fragments of previous phases in a matrix composed of quartz and fine-grained fluorite.
	9b	Late quartz	Quartz vein stockwork and vug filling.
	10	Pyrite and chalcopyrite	Pyrite and chalcopyrite crystals in quartz-lined vugs.

* Variable amounts of calcite occur locally with fluorite in all phases.

orite) and the late phases (blastonite, late quartz). Sulphides in the veins occur in two distinct phases and include sphalerite, galena, pyrite and chalcopyrite.

Early Stage (Phases 1 to 3)

The barren breccia consists of clasts of rhyolite and sedimentary rocks in a siliceous matrix. The clasts are weakly to strongly altered to tan, light and dark green due to presence of sericite and/or chlorite.

Purple fluorite typically occurs with quartz, and locally calcite, and forms either as stockwork veins in rhyolite and sedimentary rocks or as the matrix of hydrothermal breccias (Plate 13). There are at least two generations of purple fluorite, with the first one generally darker than the second. The grain size ranges from fine to medium grained, with the first generation typically being the coarser, but the opposite is observed as well. In the Open Cut Pit, purple fluorite is locally associated with sphalerite and/or galena forming fine-grained thin layers or veins. Minor light-purple fluorite cuts later phases (Plate 14), which may represent late remobilization of the purple fluorite. Coarse-grained purple fluorite also locally forms alternating layers with yellow fluorite. Fluorite content from this phase is up to 61.6% CaF_2.

The fine-grained, banded fluorite is composed of rhythmic mm- to cm-scale bands of tan, beige, pink and red fluorite, locally alternating with fine-grained white or black calcite. The colour is caused by minor amounts of fine-grained hematite. Fine-grained, banded fluorite indicates high nucleation rate and low growth rate (Dill *et al.*, 2016). This texture suggests rapid opening of a fracture and rapid precipi-

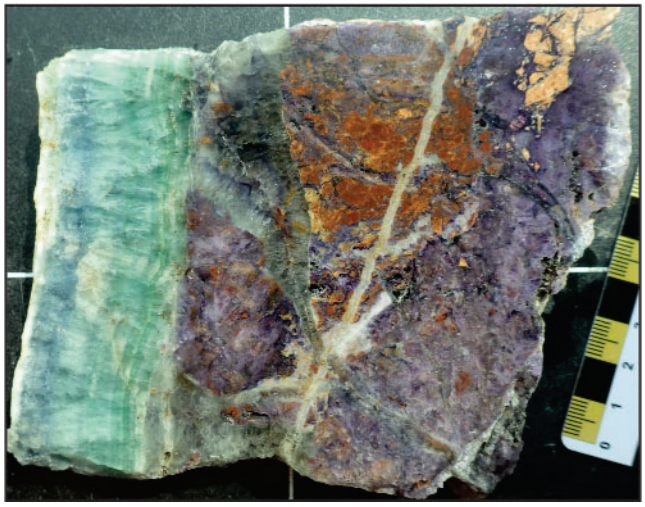

Plate 13. *Purple fluorite cut by grey fluorite, both cut by green and blue fluorite.*

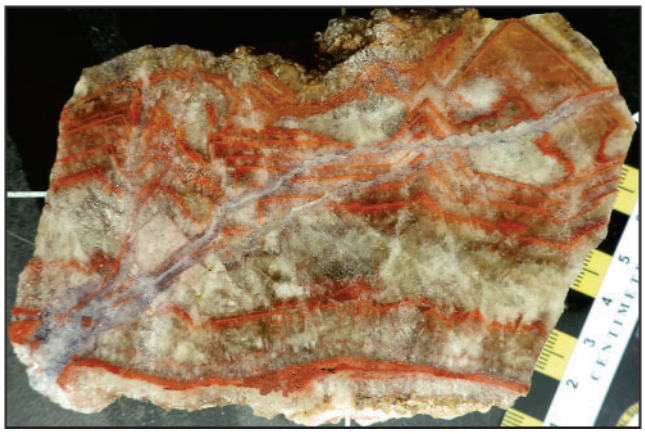

Plate 14. *Light-purple fluorite cutting massive reddish grey fluorite.*

tation of the hydrothermal mineral due to a sudden change in conditions such as temperature and/or pressure (Strong *et al.*, 1984; Henley and Hughes, 2000; Moncada *et al.*, 2012). This phase most commonly occurs after the purple fluorite phase, but it reappears in minor amounts in the main stage of fluorite mineralization (Plate 15). It likely indicates a change in the mode of crystallization (rapid vs. slow precipitation), rather than a change in composition. The grade of fine-grained, banded fluorite ranges up to 67.4% CaF_2 in samples collected from the High Carbonate Zone, where the main gangue mineral is calcite. Coarse-grained, yellow fluorite is most common in the Grebes Nest Pit. It occurs as alternating layers with the fine-grained, banded fluorite and/or coarse-grained black calcite, cubic crystals in vugs surrounded by black calcite, veins with purple fluorite; and clasts with purple and fine-grained, banded fluorite surrounded by, and cut by, later grey and green fluorite. Yellow

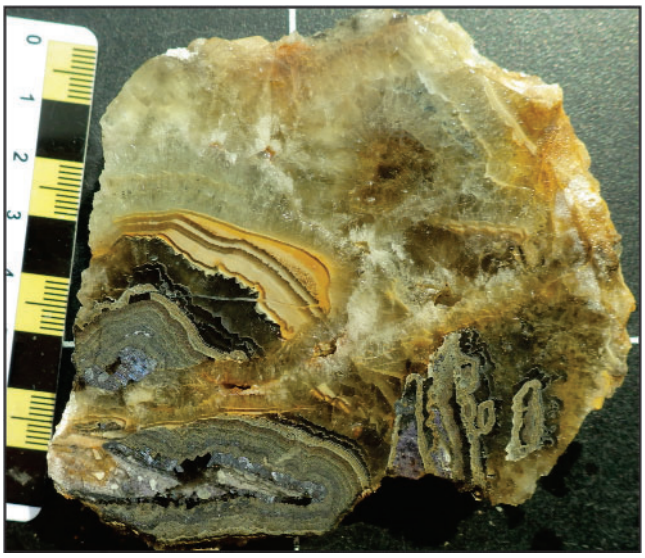

Plate 15. *Fine-grained, banded fluorite and banded sulphide in the main stage of fluorite mineralization.*

fluorite also occurs in high-grade pockets composed of lenses of yellow, clear, white and red fluorite.

Hematite–fluorite–quartz occurs in minor amounts throughout the deposit, but it is locally abundant in the Open Cut Pit and Center Pit. The relative timing of this phase is not clear, but it is interpreted to be a local variation of the fine-grained, banded and coarse-grained, yellow fluorite. In the Open Cut Pit it is composed of fibrous quartz and fine-grained hematite surrounded by quartz and fluorite. In the Center Pit, it occurs as alternating layers of hematitic quartz, white and light grey-purple fluorite and it is cut by later grey fluorite (Plate 16). It also forms layers in yellow and fine-grained, banded fluorite. This phase may persist into the grey fluorite phase, suggested by some samples from the Center Pit. The grade of the hematite–fluorite–quartz in the analyzed samples ranges up to 27.9% CaF_2.

Main Stage (Phases 4 to 6)

The main stage of fluorite mineralization is represented by the reddish grey and elongated grey fluorite phases, which are separated by an approximately 1- to 2-cm-wide-band of fine-grained sulphides composed of sphalerite and minor galena. The reddish grey fluorite is massive and coarse grained (Plate 14). The reddish colour is caused by fine-grained hematite and/or clasts of earlier hematitic fluorite. In the Center Pit, the red colour is caused by hematitic layers. The comb-textured, elongated, grey fluorite forms crystals up to 20 cm in length and indicates growth in dilatational veins in local extension zones (Plates 8, 15 and 17). These two phases occupy most of the spindle-shaped extension zone in the west end of the Grebes Nest Pit and a large

proportion of the North Vein. The CFI sampling from drillcore and select grab samples returned values between 90 and 99% CaF_2 in this phase.

Late Stage (Phases 7 to 10)

Green, blue and white fluorite is coarse to very coarse grained, ranging between 1 and 5 cm in length. They typically form alternating bands, but green fluorite is the most common. In the Grebes Nest Pit, calcite is common in this phase, occurring as alternating layers with the fluorite. Whereas most of the fluorite in the AGS deposit is cubic, green fluorite (where crystal morphology is observed) always shows an octahedral habit (Plate 18). Green and blue fluorite in all areas are associated with variable amounts of coarse-grained (~0.5 cm) galena and/or sphalerite. Galena is typically more common at Grebes Nest Pit, whereas sphalerite is more common at Open Cut Pit; but there are local variations. This phase cuts earlier phases and typically occurs in late structures oblique to the main structure hosting most of the fluorite. The CFI sampling from drillcore and select grab samples returned values between 70 and 85% CaF_2 in this phase.

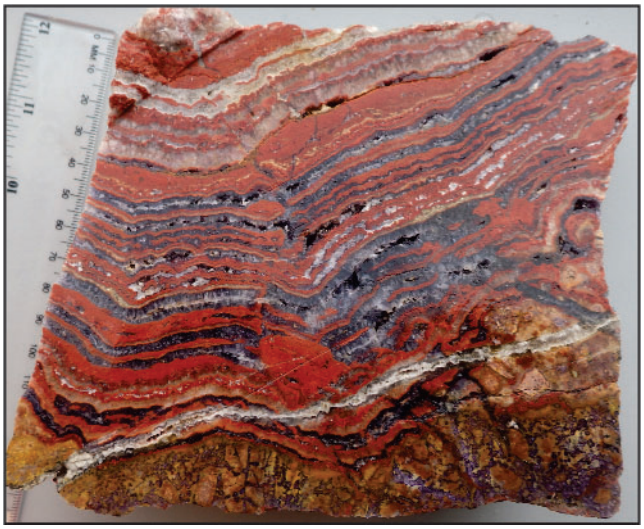

Plate 16. *Hematitic fluorite composed of layers of hematitic quartz and fluorite.*

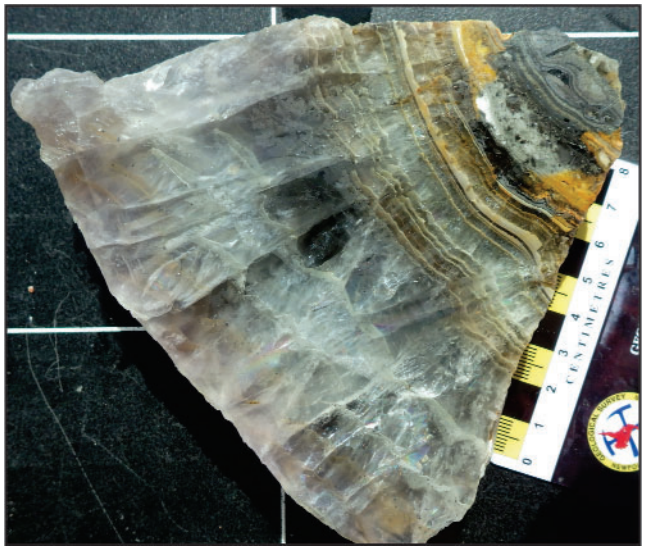

Plate 17. *Massive, elongated grey fluorite with fine-grained, banded sulphide and fluorite.*

Clear or blue, cubic fluorite occurs on top of green fluorite in vugs. The size of the cubes ranges up to 6 cm in length. The larger cubes are blue and were observed in the North Vein in vugs up to 1 m in length (Plates 19 and 20).

'Blastonite' is a local term describing a late hydrothermal event resulting in breccia composed of various sized fragments of previous mineralized phases in a matrix composed of quartz, calcite (in calcite-rich areas) and fine-grained fluorite. Quartz in the matrix commonly has a milky appearance. The blastonite results from fracturing and brecciation of previous veins during an influx of silica-rich material. Blastonite is more common in the Grebes Nest Pit. The grade of blastonite in the collected samples ranges between 15.2 and 73.2% CaF_2.

Late quartz, occurring as stockwork veins and filling vugs, is likely a variation of the blastonite and represents different environments of formation (Plate 7). Pyrite and chalcopyrite occur in quartz-lined vugs.

FLUID-INCLUSION ANALYSIS

ANALYTICAL METHODS

Detailed fluid-inclusion petrography using a petrographic microscope, and representative fluid-inclusion

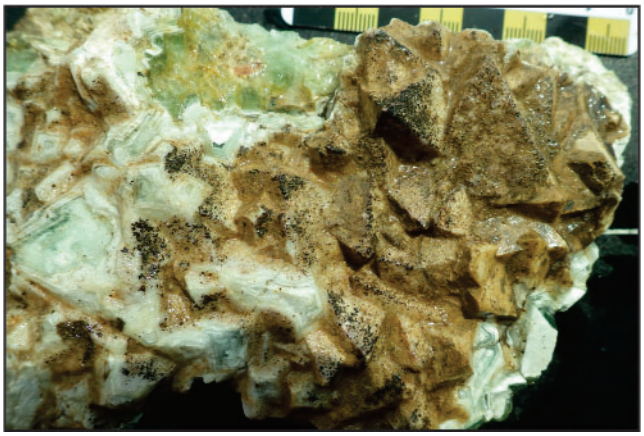

Plate 18. *Octahedral green fluorite.*

assemblages (FIA) were selected for microthermometric analysis. Microthermometric fluid-inclusion analyses at Memorial University of Newfoundland used a Linkam THMSG600 heating–freezing stage mounted on an Olympus BX51 microscope. The heating–freezing stage was calibrated using synthetic H_2O and CO_2 fluid inclusion standards at temperatures between -56.6 and 374.1°C. Precision on the measurements is ± 0.2°C at -56.6°C and ± 1°C at 300°C. Following procedures outlined by Shepherd *et al.* (1985), the temperature of homogenization (Th), eutectic melting temperature (Tm(eut)), hydrohalite melting temperature (Tm(HH) and last, ice-melting temperature (Tm(ice)) were measured in two-phase (liquid + vapour) inclusions. Homogenization temperatures were recorded first in order to minimize the effects of stretching or leaking in relatively soft minerals such as fluorite. Salinities were calculated using Tm(ice) and the equation of Bodnar (1993), which calculates salinities as equivalent weight % NaCl (eq. wt. % NaCl).

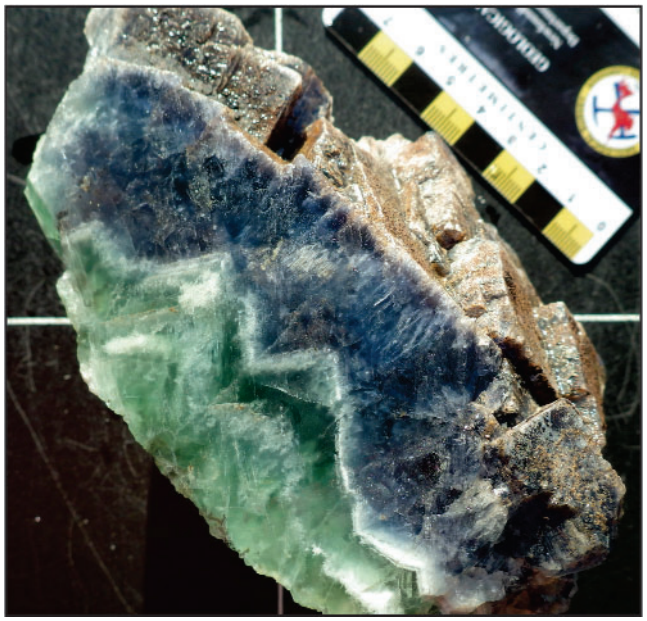

Plate 19. *Blue, cubic fluorite on top of green fluorite.*

Plate 20. *Clear, cubic fluorite on top of green fluorite.*

RESULTS

Seven samples, five from the Grebes Nest Pit and one from each of the Center Pit and Open Cut Pit, were used for fluid-inclusion analysis (Table 2). The fluorite phases included purple, yellow, green and blue fluorites. Samples from the main stage were not included, because they were not available at the time. The textures included stockwork veins and massive veins. All inclusions were two-phase liquid-vapour inclusions with a vapour to liquid ratio between 0.75 and 0.9 (Plates 21 and 22).

The homogenization temperature (Th) of the primary fluid inclusions ranges between 89.3 and 163.9°C and the

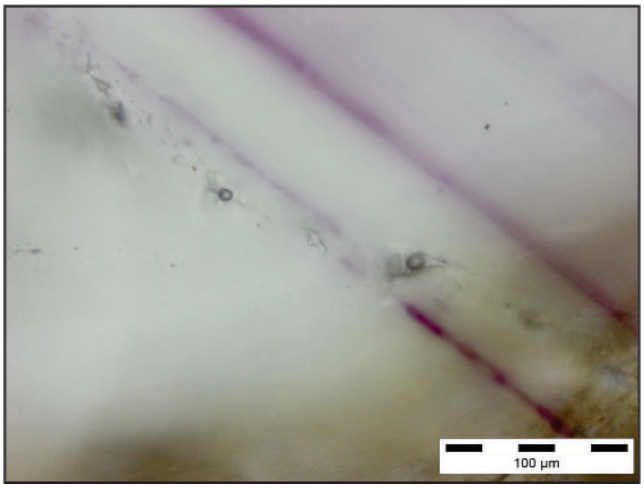

Plate 21. *Fluid inclusions in purple fluorite.*

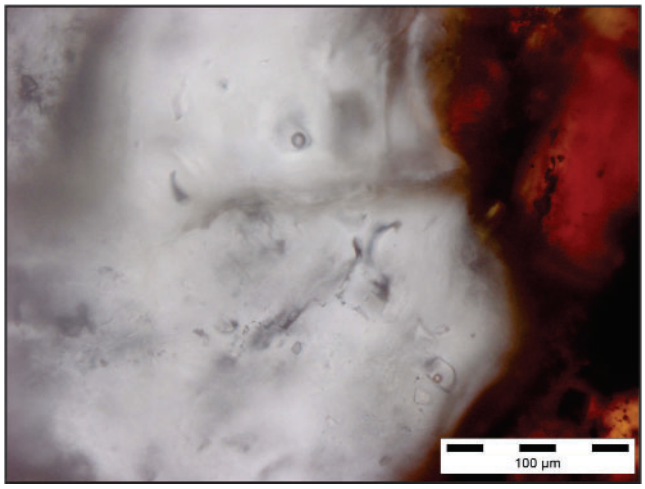

Plate 22. *Fluid inclusions in green fluorite with sphalerite (reddish brown).*

Table 2. List of samples used for fluid inclusion analysis

Sample	Location	Description
204A02	Grebes Nest Pit	Stockwork purple fluorite with calcite cut by yellow vein (at least 9 cm wide).
205A01	Grebes Nest Pit	Coarse-grained, massive, purple and yellow fluorite vein (at least 9 cm wide).
209A01	Grebes Nest Pit	Purple and minor hematitic fluorite in 3- to 4-cm-wide stockwork veins.
211A05	Grebes Nest Pit	Green fluorite with minor hematitic layers in calcite-rich breccia.
212A01	Grebes Nest Pit	Purple fluorite stockwork and hydrothermal breccia, cut by black calcite and yellow fluorite.
214A01	Open Cut Pit	Coarse-grained, green fluorite and sphalerite vein in rhyolite.
240A01	Center Pit	Purple and blue fluorite vein (more than 5 cm wide) in rhyolite.

salinity ranges between 9.47 and 27.54 wt. % NaCl equivalent (Figure 14). The Th for two fluid inclusions from a blastonite sample (211A05) with green fluorite clasts in a calcite-rich matrix were above 300°C and were concluded to have leaked. The fluid inclusions show no evidence of boiling.

In general, there is an overall trend from high salinity and lower Th fluid inclusions to low salinity and higher Th fluid inclusions, except for the yellow fluorites (Figure 14). This trend is more noticeable in some of the individual samples (209A01, 212A01 and 214A01, Figures 15, 16 and 17).

The trend in Th and salinity varies with both the colour and the texture of the fluorite (Figures 14 and 18). Earlier phases and textures are characterized by high salinity and slightly lower Th, whereas later phases and textures are characterized by low salinity and slightly higher Th. The late stage green and blue fluorites fall in the low salinity, higher Th group. The early hematitic fluorite is in the high salinity, low Th group. Most of the fluorite from stockwork veins fall in the high salinity group and most of the fluorite from massive veins fall in the low salinity group.

The trend observed in this study is similar to the trend "A" described by Strong *et al.* (1984) and Collins (1992), and it indicates mixing of high salinity magmatic liquid with low salinity liquid. Strong *et al.* (1984) suggested that the low salinity liquid originated from condensed vapour from boiling of magmatic liquid underneath, but meteoric water may have entered the system. Oxygen isotope studies indi-

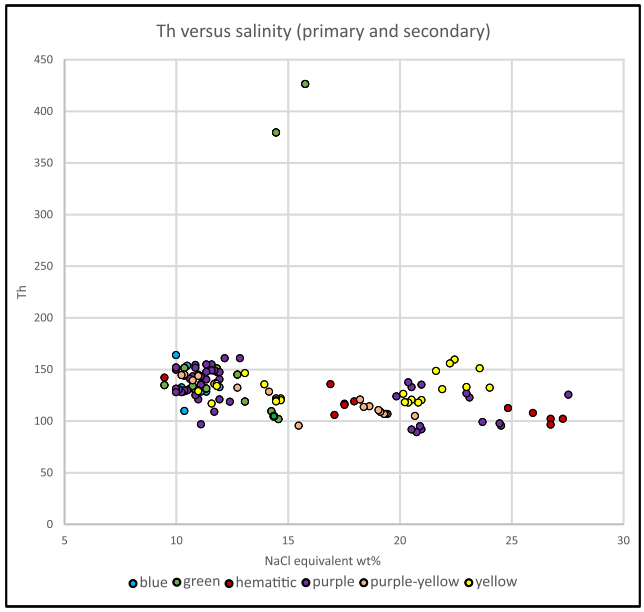

Figure 14. *Temperature of homogenization (Th)* vs. *salinity as a function of fluorite colour.*

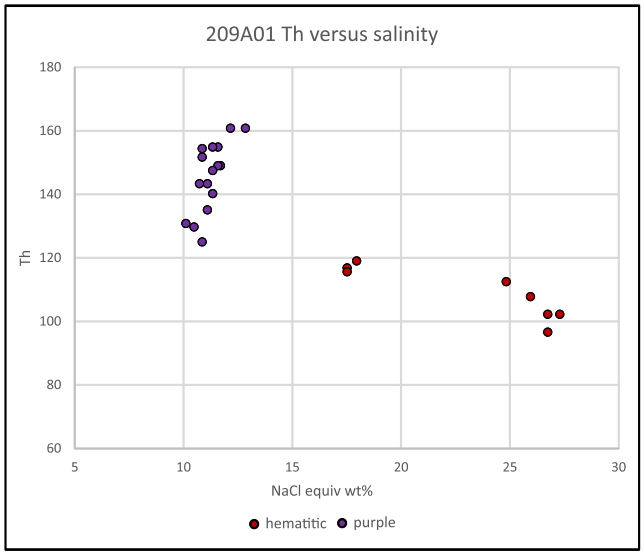

Figure 15. *Temperature of homogenization (Th)* vs. *salinity in sample 209A01.*

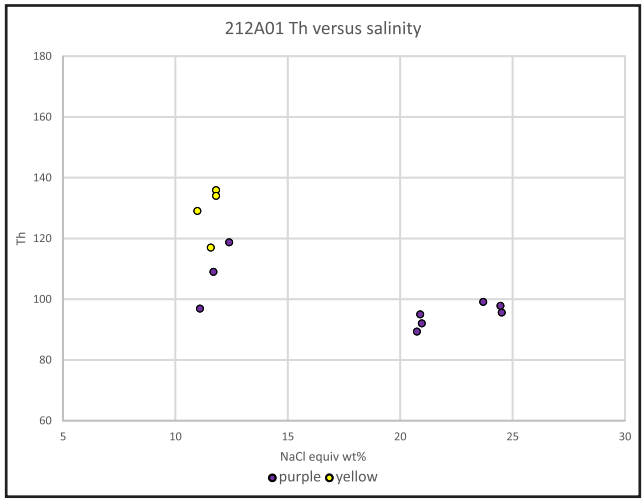

Figure 16. *Temperature of homogenization (Th)* vs. *salinity in sample 212A01.*

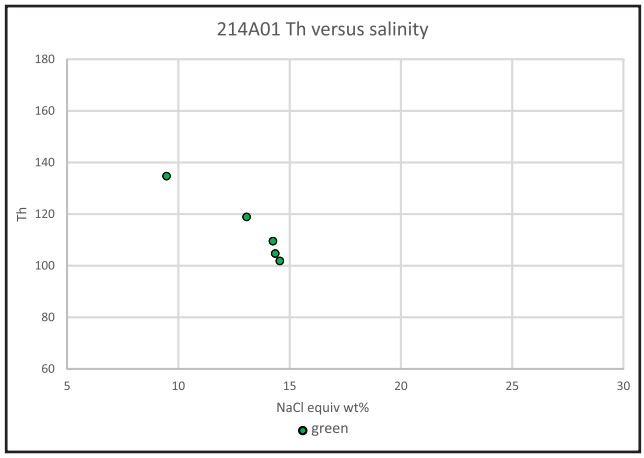

Figure 17. *Temperature of homogenization (Th)* vs. *salinity in sample 214A01.*

cate mixing of magmatic and meteoric fluids (Strong *et al.*, 1984). No evidence of boiling was found in this study.

DISCUSSION

The preliminary sequence of events that led to the formation of the AGS deposit based on data from this study is as follows: 1) deposition of the Inlet Group sedimentary rocks; 2) faulting in the sediments; 3) emplacement of the rhyolite sills; and 4) emplacement of the underlying granite.

The presence of a pre-existing fault was probably crucial to the fluorite mineralization in the AGS area. The emplacement of the rhyolite sills alone was likely not enough to allow the mineralizing fluids to escape from the underlying granite. The sedimentary rocks would have

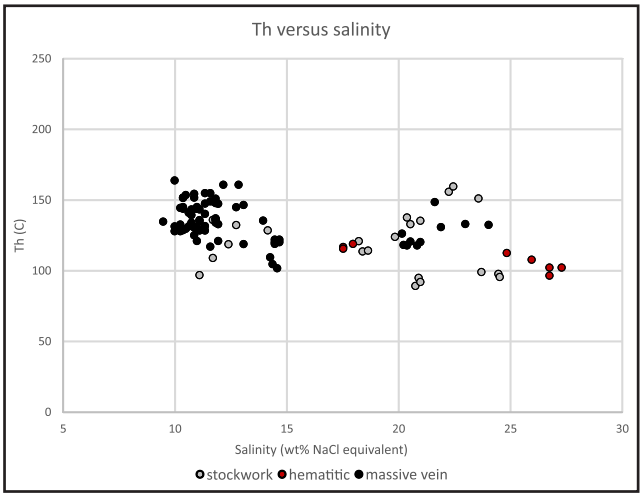

Figure 18. *Temperature of homogenization (Th)* vs. *salinity as a function of fluorite texture.*

become hornfelsed and impermeable, similar to the granite and sediment contact elsewhere. The fault was reactivated around the time of the intrusion of the SLG, which prevented ponding of the mineralizing fluids in the granite and provided channels for the fluids to migrate upward.

Repeated movement along the fault zone, during and subsequent to the emplacement of the rhyolite sills, allowed the passage of mineralizing fluids from the underlying granite and possibly the rhyolite upward in the country-rock carapace ("fault-valve model" of Sibson *et al.*, 1988). This led to multiple phases of fluorite deposition under dominantly brittle conditions. Early phases of mineralization (purple and minor yellow fluorite) are located in fault-bounded lenses, whereas the main phases of mineralization occur in extensional zones. Late phases of mineralization occur both in extensional zones, following the main phases, and in late R shears oblique to the main shear direction.

The rhyolite separated at deeper structural levels from the peralkaline granite magma and intruded along the bedding planes of the sedimentary rocks, where it cooled faster than the main body of the SLG. Fluids from the rhyolite may have provided fluorite mineralization at this time; however, the subsequent intrusion of the main phase of the SLG probably resulted in the main influx of fluorite-rich mineralizing fluids into the pre-existing fault zone.

Fluid-inclusion analysis indicates an overall trend from high salinity and slightly lower Th, characteristic of earlier phases and textures, to low salinity and slightly higher Th, characteristic of later phases and textures. This trend suggests mixing of high salinity magmatic fluids with low salinity fluids (Strong *et al.*, 1984; Collins, 1992). According to Strong *et al.* (1984), most of the low salinity

fluids originated from a condensed vapour phase following boiling, suggested by the high Th fluid inclusions analyzed in samples from some of the granite-hosted veins. Boiling led to the separation of a dense highly saline fluid and a less dense low salinity fluid (Strong *et al.*, 1984; Collins, 1992). The low salinity fluids ascended first and subsequently mixed with the high salinity fluids that ascended later. However, no evidence for boiling was found in this study, suggesting that the low salinity fluids in the AGS area were more likely meteoric fluids and not condensed vapour from boiling. This is also suggested by the change from high salinity fluid to low salinity fluid with time.

FURTHER RESEARCH

Further research will include fluid-inclusion analysis from the main stage of mineralization that were not analyzed in this study due to lack of samples at the time. This will ascertain that the findings of this study represent all phases of mineralization.

The REE and trace-element chemistry of fluorites will examine the relationship of the different fluorite phases within the granite, rhyolite and sedimentary rocks; and the nature and evolution of the mineralizing fluids.

Geochemistry and petrography of the SLG will investigate regional variations in texture and composition in different phases of the SLG, late magmatic alteration, possible origin of Ca-rich fluids outside the high carbonate zone and understand late magmatic processes that are responsible for fluorite mineralization.

ACKNOWLEDGMENTS

The first author would like to thank Alex Bugden for his enthusiastic and energetic assistance during field work in the summer. Gerry Hickey helped with providing equipment and ensuring our safety in the field. I am grateful to Mellissa Lambert, Greg Pittman, Daron Slaney and the surveyors from CFI who were extremely helpful during field work in the mine area. John Hinchey is thanked for his support and guidance throughout this project. Enlightening conversations about the project with Hamish Sandeman and Andrea Mills were really appreciated. Revision of parts of the paper by Hamish is also greatly acknowledged. Kim Morgan and Joanne Rooney assisted with the preparation of the figures and typesetting.

REFERENCES

Agangi, A., Kamenetsky, V. and McPhie, J.
2010: The role of fluorine in the concentration and transport of lithophile trace elements in felsic magmas: Insights from the Gawler Range Volcanics, South Australia. Chemical Geology, Volume 273, pages 314-325.

Allmendinger, R.W., Cardozo, N. and Fisher, D.
2012: Structural Geology Algorithms: Vectors & Tensors. Cambridge University Press, 289 pages.

Bell, K., Blenkinsop, J. and Strong, D.F.
1977: The geochronology of some granitic bodies from eastern Newfoundland and its bearing on Appalachian evolution. Canadian Journal of Earth Sciences, Volume 14, pages 456-476.

Bodnar, R.J.
1993: Revised equation and table for determining the freezing point depression of H_2O-NaCl solutions. Geochimica et Cosmochimica Acta, Volume 57, pages 683-684.

Candela, P.A.
1997: A review of shallow, ore-related granites: textures, volatiles, and ore metals. Journal of Petrology, Volume 38, Number 12, pages 1619-1633.

Cardozo, N. and Allmendinger, R.W.
2013: Spherical projections with OSXStereonet. Computers and Geosciences, Volume 51, pages 193-205.

Clemens, J.D., Holloway, J.R. and White, A.J.R.
1986: Origin of an A-type granite: Experimental constraints. American Mineralogist, Volume 71, pages 317-324.

Collins, C.J.
1984: Genesis of the St. Lawrence fluorite deposits. *In* Mineral Deposits of Newfoundland – A 1984 Perspective. Government of Newfoundland and Labrador, Department of Mines and Energy, Mineral Development Division, Report 84-3, pages 164-170.

1992: A fluid inclusion and trace element geochemical study of the granite-hosted, St. Lawrence fluorspar deposits and related host rocks. M.Sc. thesis, Memorial University of Newfoundland, St. John's.

Collins, C.J. and Strong, D.F.
1988: A fluid inclusion and trace element study of fluorite veins associated with the peralkaline St. Lawrence Granite, Newfoundland. Canadian Institute of Mining and Metallurgy, Special Volume 39, pages 291-302.

Colman-Sadd, S.P., Hayes, J.P. and Knight, I.
1990: Geology of the Island of Newfoundland. Government of Newfoundland and Labrador,

Department of Mines and Energy, Geological Survey Branch, Map 90-1.

Dill, H.G., Luna, L.I., Nolte, N. and Hansem, B.T.
2016: Chemical, isotopic and mineralogical characteristics of volcanogenicepithermal fluorite deposits on the Permo-Mesozoic foreland of theAndean volcanic arc in Patagonia (Argentina). Chemie der Erde – Geochemistry, Volume 76, pages 275-297.

Dooley, T.P. and Schreurs, G.
2012: Analogue modelling of intraplate strike-slip tectonics: A review and new experimental results. Tectonophysics, Volumes 574-575, pages 1-71.

Evans, D.T.W. and Vatcher, S.V.
2009: First, second & third year assessment report Burin Project, Licence #s 012704M, 013091M, 013119M, 013821M, 015455M, 016336M, 016461M, 016649M, 017055M, 017057M, 017059M, 017060M, 017093M, NTS 1L/13, 1L/14 and 1M/3, Burin Peninsula area, southern Newfoundland. Golden Dory Resources, Assessment Report, 44 pages.

Fortey, R.A. and Cocks, L.R.M.
2003: Palaeontological evidence bearing on global Ordovician-Silurian continental reconstructions. Earth-Science Reviews, Volume 61, pages 245-307.

Frost, B.R., Barnes, C.G., Collins, W.J., Arculus, R.J., Ellis, D.J. and Frost, C.D.
2001: A geochemical classification for granitic rocks. Journal of Petrology, Volume 42, pages 2033-2048.

Frost, B.R. and Frost, C.D.
2008: A geochemical classification for feldspathic igneous rocks. Journal of Petrology, Volume 49, pages 1955-1969.

Gagnon, J.E., Samson, I.M., Fryer, B.J. and Williams-Jones, A.E.
2003: Compositional heterogeneity in fluorite and the genesis of fluorite deposits: Insights from La-ICP-MS analysis. The Canadian Mineralogist, Volume 41, pages 365-382.

Hamilton, M.A. and Murphy, J.B.
2004: Tectonic significance of a Llanvirn age for the Dunn Point volcanic rocks, Avalon terrane, Nova Scotia, Canada: Implications for the evolution of the Iapetus and Rheic Oceans. Tectonophysics, Volume 379, pages 199-209.

Henley, R.W. and Hughes, G.O.
2000: Underground fumeroles: “Excess heat” effects in vein formation. Economic Geology, Volume 95, pages 453-466.

Hiscott, R.
1981: Stratigraphy and sedimentology of the Rock Harbour Group, Flat Islands, Placentia Bay, Newfoundland Avalon Zone. Canadian Journal of Earth Sciences, Volume 18, pages 495-508.

Irving, E. and Strong, D.F.
1985: Paleomagnetism of rocks from Burin Peninsula, Newfoundland: Hypothesis of Late Paleozoic displacement of Acadia criticized. Journal of Geophysical Research, Volume 90, Issue B2, pages 1949-1962.

Kawasaki, K.
2011: Paleomagnetism and rock magnetism of "SEDEX" Zn-Pb-Cu ores in black shales in Australia and Yukon and of fluorite veins in granite in Newfoundland. Electronic Theses and Dissertations, Paper 445, 204 pages.

Kawasaki, K. amd Symons, D.T.A.
2008: Paleomagnetism of fluorite veins in the Devonian St. Lawrence granite, Newfoundland, Canada. Canadian Journal of Earth Sciences, Volume 45, Number 1, pages 969-980.

Kerr, A., Dickson, W.L., Hayes, J.P. and Fryer, B.J.
1993a: Devonian postorogenic granites on the southeastern margin of the Newfoundland Appalachians: A review of geology, geochemistry, petrogenesis and mineral potential. *In* Current Research. Government of Newfoundland and Labrador, Department of Mines and Energy, Geological Survey Branch, Report 93-1, pages 239-278.

Kerr, A. Dunning, G.R. and Tucker, R.D.
1993b: The youngest Paleozoic plutonism of the Newfoundland Appalachians: U–Pb ages from the St. Lawrence and François granites. Canadian Journal of Earth Sciences, Volume 30, pages 2328-2333.

King A.F.
1988: Geology of the Avalon Peninsula, Newfoundland (parts of 1K, 1L, 1M, 1N and 2C). Government of Newfoundland and Labrador, Department of Mines and Energy, Mineral Development Division, Map 88-01 (coloured).

Krogh T.E., Strong D.F., O'Brien, S.J. and Papezik V.S.
1988: Precise U-Pb zircon dates from the Avalon Terrane in Newfoundland. Canadian Journal of Earth Sciences, Volume 25, pages 442-453.

Loiselle, M.C. and Wones, D.R.
1979: Characteristics and origin of anorogenic granites. Abstracts of papers to be presented at the Annual Meetings of the Geological Society of America and Associated Societies, San Diego, California, November 5–8, Volume 11, page 468.

Magyarosi, Z.
2018: Preliminary investigations of the fluorite mineralization in the sediment- and rhyolite-hosted AGS vein system, St. Lawrence, Newfoundland. *In* Current Research. Government of Newfoundland and Labrador, Department of Natural Resources, Geological Survey, Report 18-1, pages 95-121.

Mattinson, J.M.
2005: Zircon U–Pb chemical abrasion (CA-TIMS) method; combined annealing and multi-step partial dissolution analysis for improved precision and accuracy of zircon ages. Chemical Geology, Volume 220, pages 47-66.

Moncada, D., Mutchler, S., Nieto, A., Reynolds, T.J., Rimstidt, J.D. and Bodnar, R.J.
2012: Mineral textures and fluid inclusion petrography of the epithermal Ag–Au deposits at Guanajuato, Mexico: Application to exploration. Journal of Geochemical Exploration, Volume 114, pages 20-35.

Naylor, M.A., Mandl, G. and Sijpesteijn, C.H.K.
1986: Fault geometrics in basement induced wrench-faulting under different initial stress states. Journal of Structural Geology, Volume 8, pages 737-752.

Nicolas, A.
1987: Principles of rock deformation. D. Riedel Publishing Company, Dordrecht, Holland.

O'Brien, S.J., Dubé, B., O'Driscoll, C.F. and Mills, J.
1998: Geological setting of gold mineralization and related hydrothermal alteration in late Neoproterozoic (post-640 Ma) Avalonian rocks of Newfoundland, with a review of coeval gold deposits elsewhere in the Appalachian Avalonian belt. *In* Current Research. Government of Newfoundland and Labrador, Department of Mines and Energy, Geological Survey, Report 98-1, pages 93-124.

O'Brien, S.J., Dunning, G.R., Knight, I. and Dec, T.
1989: Late Precambrian geology of the north shore of Bonavista Bay (Clode Sound to Lockers Bay). *In* Report of Activities. Government of Newfoundland and Labrador, Department of Mines, Geological Survey Branch, pages 49-50.

O'Brien, S.J., O'Brien, B.H., Dunning, G.R. and Tucker, R.D.
1996: Late Neoproterozoic Avalonian and related peri-Gondwanan rocks of the Newfoundland Appalachians. Geological Society of American, Special Paper 304, pages 9-28.

O'Brien, S.J., Strong, P.G. and Evans, J.L.
1977: The geology of the Grand Bank (1M/4) and Lamaline (1L/3) map areas, Burin Peninsula, Newfoundland. Government of Newfoundland and Labrador, Department of Mines and Energy, Mineral Development Division, Report 77-7, 16 pages.

O'Brien, S.J. and Taylor, S.W.
1983: Geology of the Baine Harbour (1M/7) and Point Enragee (1M/6) map areas, southeastern Newfoundland. Government of Newfoundland and Labrador, Department of Mines and Energy, Mineral Development Division, Report 83-5, 70 pages.

O'Driscoll, C.F., Dean, M.T., Wilton, D.H.C. and Hinchey, J.G.
2001: The Burin Group: A late Proterozoic ophiolite containing shear-zone hosted mesothermal-style gold mineralization in the Avalon Zone, Burin Peninsula, Newfoundland. *In* Current Research. Government of Newfoundland and Labrador, Department of Mines and Energy, Geological Survey, Report 01-1, pages 229-246.

Papezik, V.S.
1974: Igneous rocks of the Avalon Platform. Geological Association of Canada, Annual Fieldtrip Manual B-5, 22 pages.

Pearce, J.A., Harris, N.B.W. and Tindle, A.G.
1984: Trace element discrimination diagrams for the tectonic interpretation of granitic rocks. Journal of Petrology, Volume 25, pages 956-983.

Reeves, J.H., Sparkes, B.A. and Wilson, N.
2016: Paragenesis of fluorspar deposits on the southern Burin Peninsula, Newfoundland, Canada. Canadian Institute of Mining Journal, Volume 7, Number 2, pages 77-86.

Richardson, C.K. and Holland, H.D.
1979: Fluorite deposition in hydrothermal systems. Geochimica et Cosmochimica Acta, Volume 43, pages 1327-1335.

Sallet, R., Moritz, R. and Fontignie, D.
2000: Fluorite $^{87}Sr/^{86}Sr$ and REE constraints on fluid–melt relations, crystallization time span and bulk D^{Sr} of evolved high-silica granites. Tabuleiro granites, Santa Catarina, Brazil. Chemical Geology, Volume 164, pages 81-92.

Shand, S.J.
1922 : The problem of the alkaline rocks. Proceedings of the Geological Society of South Africa, Volume 25, pages 19-33.

Shepherd, T.J., Rankin, A.H. and Alderton, D.H.M.
1985: A practical guide to fluid inclusion studies. Blackie, 224 pages.

Sibson, R.H.
1977: Fault rocks and fault mechanisms. Journal of the Geological Society, Volume 133, pages 191-213.

Sibson, R.H., Robert, F. and Poulsen, K.H.
1988: High-angle reverse faults, fluid-pressure cycling, and mesothermal gold-quartz deposits. Geology, Volume 16, pages 551-555.

Smith, W.S.
1957: Fluorspar at St. Lawrence, Newfoundland. Newfoundland Fluorspar Limited, Geological Survey Assessment Report (001L/0016).

Sparkes, B.A. and Reeves, J.R.
2015: AGS Project, project review and resource estimate, Canada Fluorspar Inc. Presentation, Baie Verte Mining Conference.

Sparkes, G.W. and Dunning, G.R.
2014: Late Neoproterozoic epithermal alteration and mineralization in the western Avalon Zone: a summary of mineralogical investigations and new U/Pb geochronological results. *In* Current Research. Government of Newfoundland and Labrador, Department of Natural Resources, Geological Survey, Report 14-1, pages 99-128.

Strong, D.F.
1982: Carbothermal metasomatism of alaskitic granite, St. Lawrence, Newfoundland, Canada. Chemical Geology, Volume 35, pages 97-114.

Strong, D.F. and Dostal, J.
1980: Dynamic partial melting of Proterozoic upper mantle: Evidence from rare earth elements in oceanic crust of eastern Newfoundland. Contributions to Mineralogy and Petrology, Volume 72, pages 165-173.

Strong, D.F., Fryer, B.J. and Kerrich, R.
1984: Genesis of the St. Lawrence fluorspar deposits as indicated by fluid inclusion, rare earth element, and isotopic data. Economic Geology, Volume 79, pages 1142-1158.

Strong, D.F., O'Brien, S.J., Strong, P.G., Taylor, S.W. and Wilton, D.H.
1976: Geology of the St. Lawrence and Marystown map sheets (1L/14, 1M/3), Newfoundland. Preliminary report for Open File release, NFLD 895, 44 pages.

Strong, D.F., O'Brien, S.J., Strong, P.G., Taylor, S.W. and Wilton, D.H.
1978: Geology of the Marystown (1M/13) and St. Lawrence (1L/14) map areas, Newfoundland. Government of Newfoundland and Labrador, Department of Mines and Energy, Mineral Development Division, Report 78-7, 81 pages.

Sun, S. and McDonough, W.F.
1989: Chemical and isotopic systematics of oceanic basalts: implications for mantle composition and processes. *In* Magmatism in the Ocean Basins. *Edited by* A.D. Saunders and M.J. Norry. Geological Society of London, Special Publication, Volume 42, pages 313-345.

Taylor, S.W.
1976: Geology of the Marystown map sheet (east half), Burin Peninsula, southeastern Newfoundland. Unpublished M.Sc. thesis, Memorial University of Newfoundland, St. John's, 164 pages.

Teng, H.C.
1974: A lithogeochemical study of the St. Lawrence Granite, Newfoundland. Unpublished M.Sc. thesis, Memorial University of Newfoundland, 194 pages.

Teng, H.C. and Strong, D.F.
1976: Geology and geochemistry of the St. Lawrence peralkaline granite and associated fluorite deposits, southeast Newfoundland. Canadian Journal of Earth Sciences, Volume 13, pages 1374-1385.

Van Alstine, R.E.
1948: Geology and mineral deposits of the St. Lawrence area, Burin Peninsula, Newfoundland.

Newfoundland Geological Survey, Bulletin Number 23, 73 pages.

1976: Continental rifts and lineaments associated with major fluorspar districts. Economic Geology, Volume 71, pages 977-987.

van Staal, C., Dewey, J., Mac Niocaill, C. and McKerrow, W.
1998: The Cambrian-Silurian tectonic evolution of the northern Appalachians and British Caledonides: History of a complex, west and southwest Pacific-type segment of Iapetus. *In* The Past is the Key to the Present. *Edited by* D. Blundell and A. Scott. Lyell, Geological Society London, Special Publication 143, pages 199-242.

van Staal, C. and Zagorevski, A.
2017: Accreted terranes of the Appalachian Orogen in central Newfoundland. Geological Association of Canada – Mineralogical Association of Canada, Field Trip Guidebook, 114 pages.

Whalen, J.B., Currie, K.L. and Chappell, B.W.
1987: A-type granites: geochemical characteristics, discrimination and petrogenesis. Contributions to Mineralogy and Petrology, Volume 95, pages 407-419.

Williams, H.
1995: Geology of the Appalachian-Caledonian Orogen in Canada and Greenland. Geological Survey of Canada, Geology of Canada, no. 6 (also Geological Society of America, The Geology of North America, Volume F1.

Williams, H., Kennedy, M.J. and Neal, E.R.W.
1974: The northeastward termination of the Appalachian Orogen. *In* Ocean Basins and Margins, Volume 2. *Edited by* A.E.M. Nairn and F.G. Stehli. Plenum Press, New York, pages 79-123.

Williamson, D.H.
1956: The geology of the fluorspar district of St. Lawrence, Burin Peninsula, Newfoundland. Government of Newfoundland and Labrador, Department of Mines, Agriculture and Resources, Unpublished report, 140 pages.

Wilson, N.
2000: Fluorspar, a guide to the mineral, veins and occurrences of the southern Burin Peninsula, Newfoundland. Government of Newfoundland and Labrador, Department of Mines and Energy, Geological Survey, Special Report, Open File NFLD/3020, 142 pages.

Wilton, D.H.
1976: Petrological studies of the southeast part of the Burin Group, Burin Peninsula, Newfoundland. Unpublished B.Sc. thesis, Memorial University of Newfoundland, St. John's.